

**A Study of Penning Ionization of Metastable Ne* and N₂O:
Potential Energy Surfaces**

by

Austin Cyphersmith

University of Pittsburgh, 2008

Submitted to the University of Pittsburgh
Honors College in partial fulfillment
of the requirements for the degree of
Bachelor of Philosophy

University of Pittsburgh

2008

**University of Pittsburgh
College of Arts and Sciences**

This thesis was presented

by

Austin Cyphersmith

It was defended on
April 17, 2008
and approved by

Michael Golde, Professor, Chemistry

Susan Graul, Professor, Chemistry

Rainer Johnsen, Professor, Physics

Thesis Director: Peter Siska, Professor, Chemistry

A Study of Penning Ionization of Metastable Ne* and N₂O:

Potential Energy Surfaces

Austin Cyphersmith

University of Pittsburgh, 2008

Penning Ionization Electron Spectroscopy (PIES) was used to study the reaction of metastable Ne* and N₂O. Crossed, supersonic molecular beams were used to deliver the reagents to each other. Tentative peak assignments were made for the spectra obtained for two collision energies, 0.075eV and 0.136eV. The reaction was performed over a range of kinetic energies from 0.3eV to 4.0eV. The X state peak was found to be blue shifted by 0.01eV and the A state was found to be blue shifted by 0.04eV. This shift was used to make qualitative inferences about the nature of short range forces between the Ne* and N₂O molecules up until the time of collision.

Table of Contents

| | |
|---------------------------------------------------------|----|
| Introduction..... | 7 |
| Theory..... | 12 |
| The Penning Ionization Reaction..... | 12 |
| Electron Spectroscopy..... | 17 |
| Collision Theory..... | 19 |
| Two Potential Model..... | 24 |
| Potential Energy Surfaces..... | 29 |
| Experimental..... | 35 |
| Overview..... | 35 |
| Supersonic Beams..... | 35 |
| Preparation of Reagent's Internal Energy..... | 37 |
| Production of Ne* and Electron Gun..... | 39 |
| Vacuum System and Main Chamber..... | 42 |
| Electron Analyzer..... | 42 |
| Data Analysis..... | 48 |
| Calibration..... | 48 |
| Raw PIES Transmission Correction..... | 48 |
| Peak Shifts..... | 50 |
| Relative Populations..... | 53 |
| Vibrational Progressions..... | 54 |
| Conclusions..... | 55 |
| Appendix..... | 57 |
| A-1 Franck-Condon Approximation..... | 57 |
| A-2 Complex Potentials..... | 58 |
| A-3 Vibrational Analysis of N ₂ O..... | 60 |
| A-4 Properties of Target Molecule N ₂ O..... | 61 |
| A-5 List of Equipment..... | 63 |
| References..... | 64 |

List of Figures

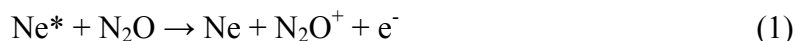
| | |
|-----------------------------------------------------------------------------------------------------------------------------------------------------------------------------------------------------------------------------------------------------------------------------------------|----|
| Figure 1: Exchange Mechanism for Penning Ionization. Using Ne^* and N_2O . This diagram illustrates an electron being ejected from the X state of N_2O | 15 |
| Figure 2: The mechanism for the Auger process. Note the similarity to the exchange mechanism for Penning Ionization. | 15 |
| Figure 3: Illustration of hard sphere scattering. The impact parameter is denoted by b and the scattering angle is denoted by θ | 20 |
| Figure 4: Illustration of scattering with non-contact forces. The impact parameter is denoted by b and the scattering angle is denoted by θ | 20 |
| Figure 5: Illustration of impact parameter's effect on the solid angle (Ω) and cross section. | 20 |
| Figure 6: V_{eff} plotted versus r for a number of b . This demonstrates the effect of an increasing centrifugal barrier on the effective potential energy. | 22 |
| Figure 7: Transition between V_0 and V_+ | 22 |
| Figure 8: Illustration of the zero crossing point. An imaginary potential Γ is added in order to account for the probability of reaction. This is described in detail in Appendix A2..... | 26 |
| Figure 9: The reaction is indicated by the vertical line. For a blue shift the reaction occurs to the right of the zero crossing point and for a red shift the reaction occurs to the left of the zero crossing point. | 26 |
| Figure 10: The difference in hill position for attractive and repulsive forces for a typical reaction. | 33 |
| Figure 11: This is the potential energy curve for the Penning Ionization reaction. A is Ne^* and BC is N_2O . After the reaction, C would be the electron and AB is an NeN_2O^+ complex just before dissociation..... | 33 |
| Figure 12: The general setup of the main chamber and beam sources. | 36 |
| Figure 13: The location of the diffusion pumps for the vacuum system. | 37 |
| Figure 14: Schematic of the electron gun. | 41 |
| Figure 15: Circuit diagram for the electron gun. | 41 |
| Figure 16: An illustration of how an Einzel lens works to focus electrons. The inner and outer lenses are kept at different voltages which focus the electrons just as an optical lens focuses photons. | 44 |
| Figure 17: Circuit diagram for the Einzel lens and related electronics. | 44 |
| Figure 18: Rough diagram of the electron analyzer. | 45 |
| Figure 19: HeI calibration spectrum with the $\text{Ne}^* + \text{N}_2\text{O}$ reaction with a collision energy of 0.075eV. The HeI peak is located at 4.56eV. | 49 |
| Figure 20: HeI calibration spectrum with the $\text{Ne}^* + \text{N}_2\text{O}$ reaction with a collision energy of 0.136eV. The HeI peak is located at 4.56eV. | 49 |
| Figure 21: $\text{Ne}^* + \text{N}_2\text{O}$ PIES spectrum with a collision energy of 0.075eV. The X state is located at 3.74eV and the A state is located at 0.28eV. | 51 |
| Figure 22: $\text{Ne}^* + \text{N}_2\text{O}$ PIES spectrum with a collision energy of 0.136eV. The X state is located at 3.74eV and the A state is located at 0.26eV. | 51 |
| Figure 23: Lewis structure for N_2O . The asymmetry indicates a dipole moment that is lacking in CO_2 | 62 |
| Figure 24: Electron configuration for N_2O . Electrons removed from the valence shell belong to non-bonding pi orbitals. Ionization of the 2π orbital produces the X state of N_2O . Ionization of the 4σ orbital produces the A state. | 62 |

List of Tables

| | |
|--------------------------------------------------------------------|----|
| Table 1: Excitation energies for He and Ne..... | 52 |
| Table 2: Adiabatic Ionization Potentials for N ₂ O..... | 52 |

Introduction

The focus of this paper is to study the Penning Ionization reaction:



in terms of both the theory of Penning Ionization and the dynamical information concerning the reaction. Penning Ionization is a special case of chemionization in which a target molecule is ionized by an excited molecule.

To truly understand a reaction it is necessary to have a good idea of what the potential energy surface for the reaction looks like. This allows an attempt at solving the Schrödinger equation for the system which provides the dynamical information for the reaction. Obtaining a potential energy surface for a reaction is not an easy task. Fortunately much of the requisite theory necessary to accomplish this with regards to Penning Ionization reaction has been developed since Penning Ionization's discovery in 1927 by Francis Penning.¹

In 1927, F.M. Penning discovered Penning Ionization during his research with noble gases. Specifically, he found that adding impurities to Ne or Ar gas would result in premature electric discharge of the gases.² This occurred due to an additional ionization source – metastable noble gases undergoing the Penning Ionization reaction. Jesse and Saudaskis would later (1952) credit the Penning Ionization reaction for the increase in ionization due to addition of noble gas impurities in their experiments. Actually, the

¹ F.M. Penning; *Naturwissenschaften*, 1927, **15**, 818

² *Molecular-beam studies of Penning Ionization*, P.E. Siska, Rev. Mod. Phys., Vol 65, No. 2, April 1993, page 337

Penning Ionization reaction is a specific case of the Jesse effect³. In which a gas ionizes at a lower temperature than normal upon the addition of impurities with a lower ionization potential. Penning Ionization is the case in which the impurity is a noble gas atom.

In 1966, Cermak, Herman⁴, Shoulette, and Muschlitz⁵ applied molecular beam techniques to the study of Penning Ionization reactions. These experiments of the Penning Ionization reaction between He* and various small polyatomic molecules laid the ground work for similar future experiments. The research of Penning Ionization Electron Spectroscopy (PIES) yielded the development of a theory and a powerful analytic technique for studying molecules. The PIES technique would be used to further study Penning Ionization reactions, but it would also be used to study target molecules themselves.

The study of Penning Ionization led to the development of a theory describing it. The Penning Ionization reaction was described via a two potential model, proposed by Cermak and Herman⁶, which would become essential in studying the reaction. Studies by Brion confirmed that the electronic spectra produce via Penning Ionization had similar Franck-Condon factors as spectra produced by photo ionization. Research by Hotop would lead to PIES using purely triplet states of He; he would also perform the first temperature dependent studies of Penning Ionization⁷. Later, Ohno's research⁸

³ *Experimental Techniques in High-Energy Nuclear and Particle Physics*; Thomas Ferbel; 1991; World Scientific

⁴ *The Collision Dependence of Penning Ionization of Nitrogen Molecules by Metastable helium as Determined by Electron Spectroscopy*; Dunlavy; PhD. Thesis; University of Pittsburgh; 1996

⁵ *Molecular-beam studies of Penning Ionization*, P.E. Siska, Rev. Mod. Phys., Vol 65, No. 2, April 1993, page 337

⁶ *Penning Ionization and Related Processes*; Yenchu; Dept Chem; NY State University at Albany; 1984

⁷ *The temperature dependence of penning ionization electron energy spectra: He(2³S)-ar, N₂, NO, O₂, N₂O, CO₂*, Hotop, H., Kolb, E., Lorenzen, J., Journal of Electron Spectroscopy and Related Phenomena,

established the ionization cross section's dependence on temperature (molecular kinetic energy). The research performed by these individuals (and others) helped to construct a working theory of the Penning Ionization reaction; the classical version of this theory is explained and used thoroughly in this thesis.

This apparent burst of PIES research beginning in 1966 can be attributed to the refinement of molecular beam techniques. Though the Penning Ionization reaction was known for some time it was not until the development of molecular beam techniques that the proposed mechanism, $A^* + B \rightarrow A + B^+ + e^-$, could be tested. Furthermore, molecular beams are useful for studying Penning Ionization because they provide an excellent means of studying reactions involving metastable atoms. Due to the nature of delivery of the reactants to one another the technique is absolutely essential in studying reactions with short lived species.

A molecular beam is based on an idea of molecular kinetics which suggests that at low pressures gas molecules move in straight lines. This makes sense if we think about the mean free path of a gas molecule. If a gas is at low pressure there are very few gas molecules in a given area and the chances that they will collide is lower than if the gas had been at a higher pressure. Suppose we have the pressure so low that the mean free path of the gas molecules is about 1 meter. If our vacuum chamber is a dimension smaller than a meter, then on average it is unlikely for the gas molecules to interact with one another. We could conceive of doing experiments using short lived reagents that are charged, radical, or excited. As long as the reagent cannot decay on its own we should have no problem using it.

16 (3), pages 213-243, 1979
⁸ *State-resolved collision energy dependence of Penning ionization cross sections for N₂ and CO₂ by He*2³*; Ohno, Takami, Mitsuke; Journal of Chemical Physics; Vol 94; page 2675; 1991

This technique took considerable time to develop and even more time to refine. One of the earliest (but certainly the most famous) uses of a molecular beam was the Stern-Gerlach experiment (1922) in which a beam of silver atoms was used to prove that particles have intrinsic angular momentum. Stern continued research within the field of molecular beams well into his retirement.⁹ Meanwhile, molecular beam techniques were refined and were applied to study chemical systems; these techniques aided in the development of the fields of NMR, laser spectroscopy, and molecular collisions. The latter would lead to the development of the theory of Penning Ionization.

With the development of a proper theory, Penning Ionization electron spectroscopy moved from being a subject of inquiry to a useful tool for studying molecular reactions. PIES has been applied to the study of large, more complex target molecules. For example, within the past decade PIES has been used by Hotop, Hansen, Weber, and others to study novel molecules such as fullerenes (C_{60} and C_{70}). PIES has also found applications in the study of surfaces and thin chemical films. Penning Ionization is also of interest in the field of plasma physics for some time. This interest is due in part to the fact that Penning Ionization reactions often involve an AB^+ complex with a large ionization cross section; as a result, the presence of these reactions in plasmas is not trivial.¹⁰ In the field of plasma physics, Penning Ionization is an accepted mechanism for the production of plasma from a metastable species. Penning ionization finds a place in the field of electron spectroscopy. Instead of using x-ray or Auger processes to induce the ionization of a target molecule the Penning mechanism can be used. Progress in these experiments can be slow, due in part to spectrum complexity

⁹ *Atomic and Molecular Beams: The State of the Art*; Roger Campargue; 2000

¹⁰ *Plasma Physics and Engineering*; Alexander A. Fridman, Lawrence A. Kennedy; 2004; Taylor and Francis ;page 35

increasing dramatically with increased molecule size. This problem will become apparent later in this paper even three atom target molecules can produce spectrums that are difficult to interpret.

Theory

The Penning Ionization Reaction

A Penning Ionization reaction occurs as follows:



where A^* is a metastable molecule and B is a ground state molecule. In this context a metastable molecule is a molecule in an excited electronic state that persists for a longer time than a typical excited state molecule (this means the excited state cannot undergo spontaneous optical emission). This lingering effect is typically due to a forbidden transition from the excited electronic state to the ground electronic state (forbidden transitions in this research will be discussed in experimental section). With noble gas excited states (the state and the state in particular) the length of time for the excited state to exist is sufficiently long enough for the metastable reagent to be used in the experiment.

The Penning Ionization reaction described above is similar to the well known photoelectric effect. In the photoelectric effect a photon impinges on a metal. If the photon has a sufficient amount of energy (i.e. is above a certain frequency) then an electron will be ejected from the metal. The electron is ejected with a kinetic energy, E , given as:

$$E = h\nu - \phi \quad (3)$$

where ϕ is the work function of the metal, ν is the frequency of the photon, and h is Planck's constant. The work function is the binding energy of the electron. The same idea is at work with Penning Ionization. The difference is that the energy used to overcome the work function is provided by a metastable atom and the work function is

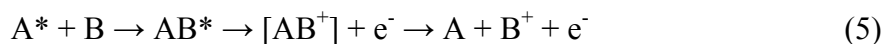
the ionization energy of the target molecule. To get an idea of what we can learn from this process we need to look at the mechanism of the Penning Ionization reaction.

Penning Ionization is also a bit more complicated than the photoelectric effect due to the presence of multiple reactions that can occur between the reagent molecules. Indeed other reactions ionization reactions do occur. The most common of these reactions is the associative ionization reaction:



where the A^* and B reagents stick together in an inelastic collision. This reaction will occur when the kinetic energy of A^* is enough to eject an electron but not enough to break away from the target molecule. This results in an inelastic collision between molecules.

This reaction is actually not entirely different from the Penning Ionization (discussed below). In fact the AB^+ system is a transition state for the typical Penning Ionization reaction:



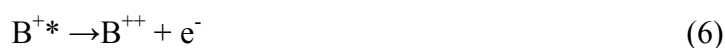
The idea of the AB^+ transition state being part of the mechanism for Penning Ionization is supported by the Franck-Condon approximation (see Appendix A-1). This approximation says that electronic transitions – like ejecting an electron – occur very quickly relative to nuclear transition – like molecular vibrations. If the electron is ejected quickly from the AB^+ system then it is a safe bet that the nuclear arrangement of atoms is stationary while this happens. Of course the AB^+ state will decay into the $A + B^+$ state and this happens soon after the electron is ejected.¹¹

¹¹*Molecular-beam studies of Penning Ionization*, P.E. Siska, Rev. Mod. Phys., Vol 65, No. 2, April 1993, page 337

The generally accepted mechanism for the Penning ionization reaction is the exchange mechanism¹² and occurs as follows. First, consider a complex, AB* (as in the associative ionization mechanism). A is noble gas particle (e.g He $1s^1 2s^1, 2^1S_0$) and the other a neutral target molecule B; the complex is in an excited state with the excitation occurring in the noble gas particle. The excited noble gas atom now has a hole in the lower orbital. When the target molecule collides with the excited noble gas atom the molecular orbitals are allowed to overlap. Electrons can now be transferred between the orbitals; specifically an electron from the target molecule's orbital falls into the hole of the noble gas atom's lower orbital. Following this electronic transition, the electron in the upper orbital of the noble gas atom is ejected into an energy continuum – the electron goes from a bound to a free state. The resulting products are a noble gas atom, an ion, and a Penning electron. (See Figure 1).

This mechanism suggests that the Penning Ionization reaction is spontaneous only in the case where molecular orbitals of the target molecule are at a higher energy than the hole in the noble gas atom. This restricts the probing power of Penning Ionization to the outer most molecular orbitals.

If this mechanism looks familiar that is because this process is similar to Auger electron spectroscopy. Auger electron spectroscopy occurs in the following fashion. A source of ionization energy, an electron or an x-ray, impinges on a target molecule, B. If the energy is sufficient to eject a core electron from the target molecule this results in a molecule B⁺*. This molecule is unstable and quickly decays via the reaction:



¹²*Doubly Differential Reactive Scattering In Molecular Penning Ionization Systems*, 2005, Keerti Gulati, Univ. Pitt, Thesis page 3-5

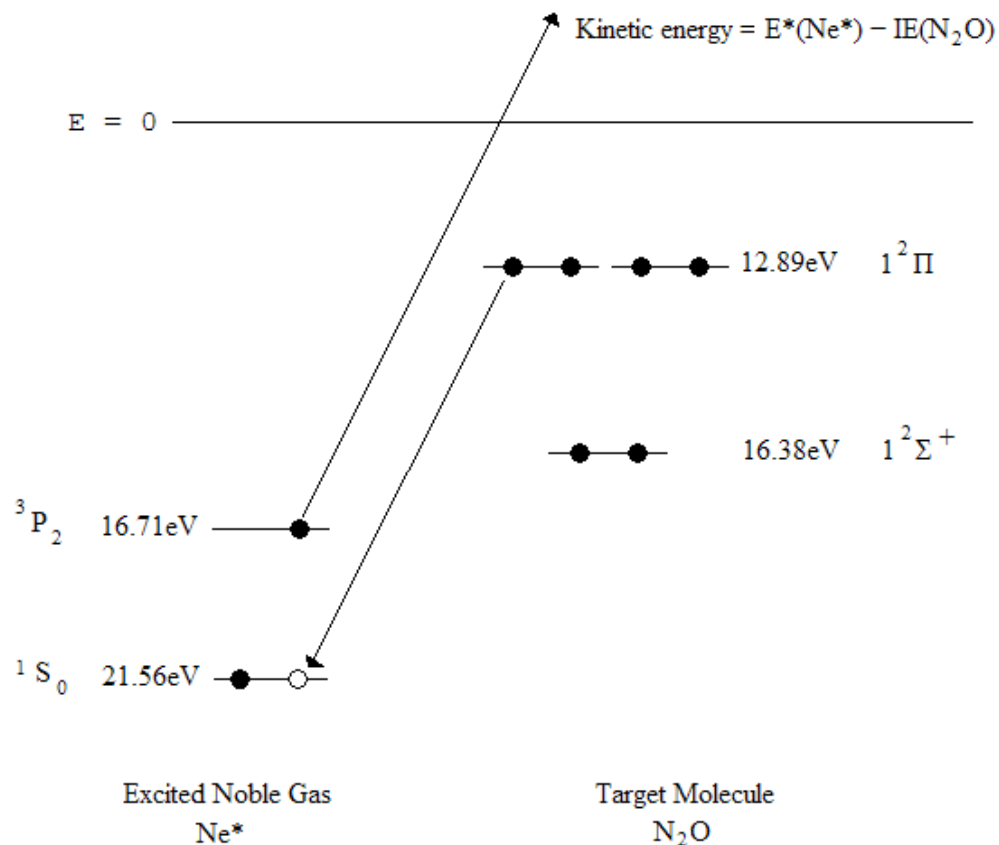


Figure 1: Exchange Mechanism for Penning Ionization. Using Ne* and N₂O. This diagram illustrates an electron being ejected from the X state of N₂O.¹³

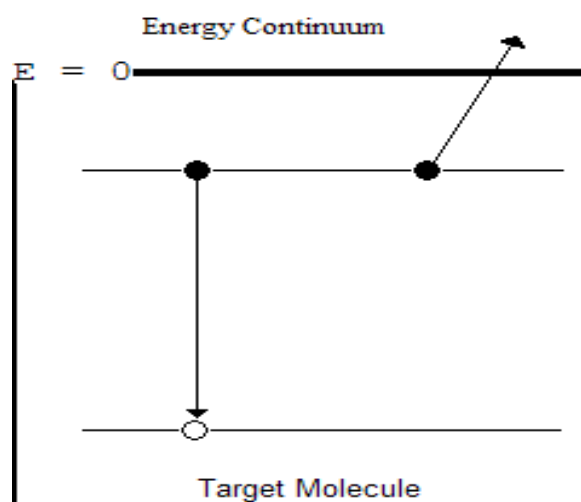


Figure 2: The mechanism for the Auger process. Note the similarity to the exchange mechanism for Penning Ionization.

¹³ <http://physics.nist.gov/PhysRefData/IonEnergy/tblNew.html>

resulting in one of the valence electrons falling to fill the hole in the core and subsequently ejecting another valence electron (see Figure 2). The mechanism is much the same in Penning Ionization. The difference is only that the hole is created by exciting an atom to a metastable state in lieu of electron removal. The hole is filled by an electron from a higher energy orbital in the target molecule rather than a valence orbital. Penning Ionization is indeed a sort of intermolecular Auger spectroscopy.

Auger electron spectroscopy is useful experimentally because the Auger electron has a kinetic energy that is reflective of the orbital it was ejected from. The same is true of Penning ionization. The Penning electron has a kinetic energy that is reflective of the energy of the target molecule's molecular orbital from which it is ejected. This will be discussed later in the section regarding the two potential model.

So how do we observe any useful information from a Penning Ionization reaction? I have already suggested that the Penning electron is much like the Auger electron in that the kinetic energy of the electron depends on the energy of the orbital from which it was ejected. This suggests that we can observe the information about the ionization energy of the target molecule by observing the electron kinetic energy. Indeed looking at ejected electrons is how any quantitative or qualitative information is obtained.

The goal of this thesis is to obtain information regarding the potential energy of the target molecule and metastable system. Since we cannot measure the potential energy directly we should do the next best thing and measure the electron kinetic energy. As will be explained in the coming sections, the aspects of the potential energy surface between the target molecule and the metastable can be inferred from electron kinetic energies. Before we can infer anything we need an explanation of electron spectroscopy.

Electron Spectroscopy

Electron spectroscopy is of vital importance to the subject of Penning Ionization - it plays the role of our eyes in observing the reaction. An electron spectrum is a plot of electron population (counts of electrons) versus the kinetic energy of electrons. Electron spectroscopy is widely used in the study of x-ray and Auger processes. In fact photoelectron spectroscopy can be used for any number of ionizing sources. Specific to this research is HeI (excited Helium) photoelectron spectroscopy. In this case photons ejected from excited Helium deliver the ionizing energy to a target molecule, ejecting an electron. HeI photoelectron spectroscopy is well studied and will be used as a means of calibration for this research.

Each electron of the target molecule is bound to a molecular orbital. In order to remove an electron from an orbital a specific amount of ionization energy must be supplied. (It is not technically correct to equate the molecular orbital energy and the ionization energy, however, as suggested by Koopman's Theorem they are approximately equal.) When the electron is removed from the orbital it will be unbound and will have a kinetic energy. The kinetic energy of the ejected electron is approximately equivalent to the energy difference between the ionization potential and the excitation energy of the metastable.¹⁴ This is again very similar to the case of the photoelectric effect; in this case the work function is the energy of the molecular orbital and the kinetic energy is the difference of the work function and the ionization energy.

I have been speaking as though we are only using one HeI photon to probe one and molecule and study one electron. In reality, will use countless HeI photons to probe

¹⁴*Principles of Instrumental Analysis*, Skoog, Holler, Nieman; Brooks/Cole; 5th Ed.; page 543-545

countless molecules and observe the ejected electrons. There will be certain kinetic energies that are heavily populated with electrons. These peaks of electron counts are representative of ionization energies. An electron spectrum provides us with a listing of the numerical values for the ionization energies of the target molecule.

While any of the molecular orbitals could give up an electron during a collision, it really only makes sense to consider the first few orbitals. The lower the energy of the molecular orbital the more energy required to eject an electron from that orbital. When an electron is removed from the HOMO (highest occupied molecular orbital) of the molecule the energy of the molecule is different than when an electron is removed from the HOMO-1 orbital. In order to properly refer to the particular state of a molecule we have to refer to which orbital the electron was ejected from. For this it is common practice to refer to an electron ejection from the HOMO as the X state, an electron ejection from the HOMO-1 as the A state, an electron ejection from the HOMO-2 as the B state and so on.

There is an incorrect assumption in the idea that the electron spectrum gives an accurate representation of the molecular orbital energies. I have assumed that the ejected electron is unaffected by the potential energy between the two incident metastable and the target molecule. This is not the case. Indeed the ejected electrons will show shifts in their kinetic energy due to potential energy of the molecules. To understand how the potential energy of the nuclei affects the electron kinetic energy we need to consider collision theory and the two-potential model.

Collision Theory

To understand the relationship between the total energy of the system and the potential energy of the system a review of basic collision theory is in order. Consider the case of hard sphere scattering. An image, Figure 3, of the scattering is provided.¹⁵

Here the impact parameter – how close the collision is – is given the symbol b . There is also a scattering angle, θ .

The hard sphere case is good for introducing the variables needed to describe the collision. However, it does not present a very realistic model. In fact the hard sphere model represents a potential surface that is zero everywhere except at the points where the sphere target sphere exists – where the potential is infinite. In reality the potential surface for the collision should be more gradual and the spheres will not act only through contact forces. For a gradual and continuous potential, even if the impinging sphere does not directly hit the target it will be swayed off course as shown in Figure 4.¹⁶

This is analogous to the case in astronomy when an unbound comet approaches a star – the comet bends around the star as it approaches and then goes off to infinity.¹⁷ With this in mind it would seem that the scattering angle depends on the potential well that is experienced by the impinging molecule. Furthermore, as shown in the hard sphere scattering image above, the scattering angle is dependent on the impact parameter. Consequently the impact parameter depends on the potential energy of the target.

To better understand the relationship between the impact parameter and the potential energy it helps to look at the energy of the system. During a collision the

¹⁵ *Classical Mechanics*; John Taylor; University Science Books; 2004; page 559

¹⁶ *Classical Mechanics*; John Taylor; University Science Books; 2004; page 559

¹⁷ *Classical Mechanics*, John Taylor, University Science Books; 2004; page 305

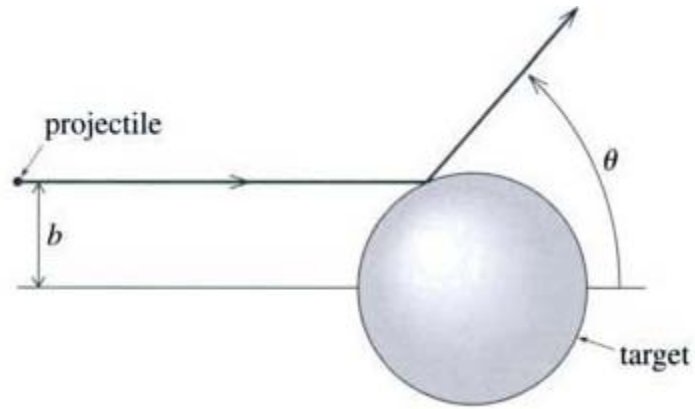


Figure 3: Illustration of hard sphere scattering. The impact parameter is denoted by b and the scattering angle is denoted by θ .

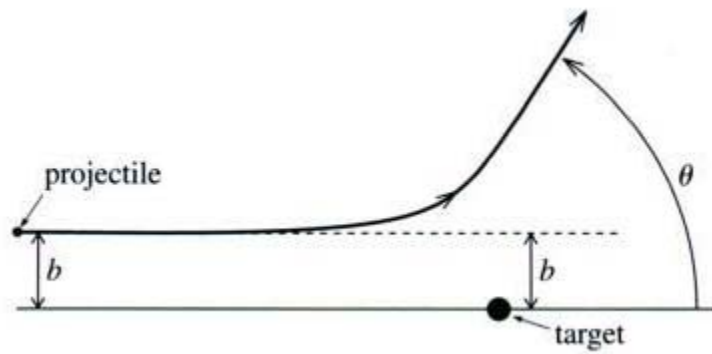


Figure 4: Illustration of scattering with non-contact forces. The impact parameter is denoted by b and the scattering angle is denoted by θ .

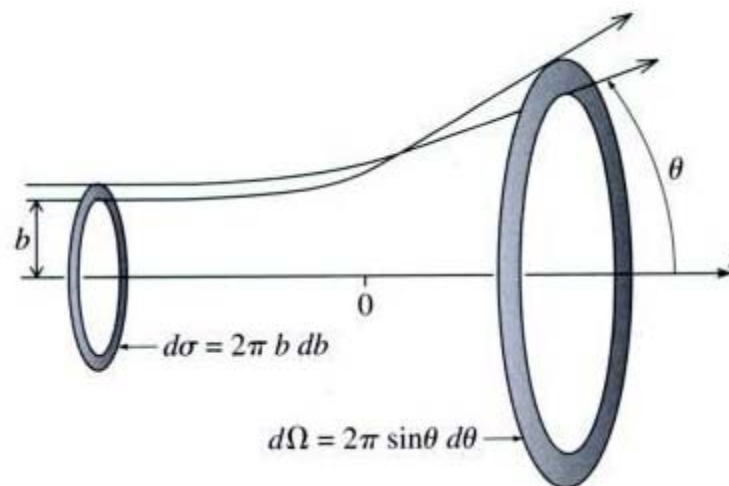


Figure 5: Illustration of impact parameter's effect on the solid angle (Ω) and cross section.

molecules have and total energy given by equation 7:

$$E_{\text{tot}} = T + V \quad (7)$$

V is the potential energy of the system and T is the kinetic energy. The kinetic energy has a radial component, $\frac{1}{2}\mu(\text{dr}/\text{dt})^2$. There is also a centrifugal component of the kinetic energy, $\frac{1}{2}E_{\text{tot}}(b/r)^2$. (There may be disagreement about the use of the term centrifugal, however, within the field of molecular reaction dynamics this is the name that has stuck.) The main relation between the impact parameter and the potential energy is expressed by the centrifugal energy of the system. As two molecules experiencing an attractive force are brought together they will begin to rotate around each other given that they have enough kinetic energy. This rotation is the centrifugal energy of the system. This is again analogous to the astronomical case of a satellite orbiting a planet. The satellite will not collide with the planet so long as it has a certain kinetic energy. This centrifugal barrier will play a more pronounced role in intermolecular collisions where there is a short range repulsive force between the molecules in addition to a long range attractive force. Once the centrifugal term is considered, the total kinetic energy can be written as:

$$T = \frac{1}{2} \cdot \mu \cdot \left(\frac{\text{d}r}{\text{dt}} \right)^2 + \frac{1}{2} \mu \cdot \left(\frac{\text{d}r}{\text{dt}} \right)^2 \cdot \left(\frac{\text{d}\theta}{\text{dt}} \right)^2 \quad (8)$$

It is more illuminating to view the centrifugal barrier as part of an effective potential energy. Having grouped the centrifugal energy into an effective potential, we can write the effective potential as:

$$V_{\text{eff}} = V(r) + E_{\text{tot}} \left(\frac{b}{r} \right)^2 \quad (9)$$

where b is the impact parameter. It is easy to see from this equation that the impact parameter will have a direct effect on the potential energy experienced by the molecules.

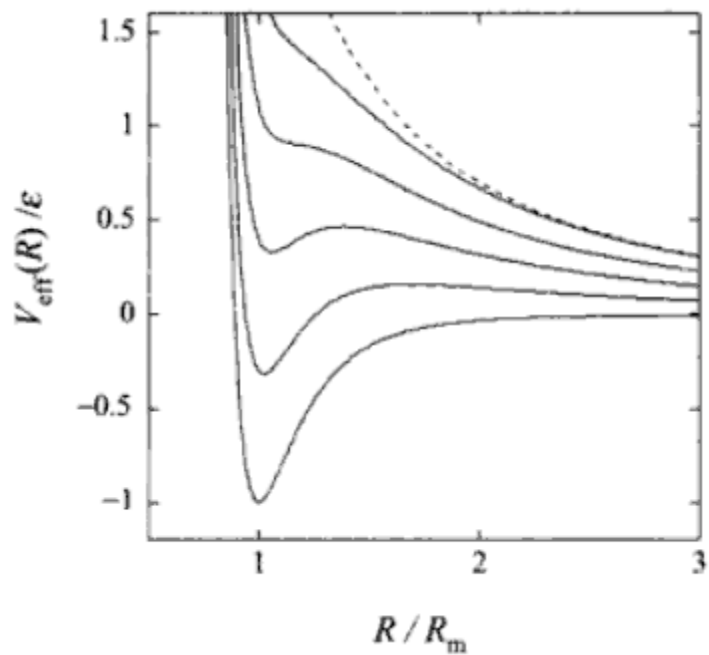


Figure 6: V_{eff} plotted versus r for a number of b . This demonstrates the effect of an increasing centrifugal barrier on the effective potential energy.

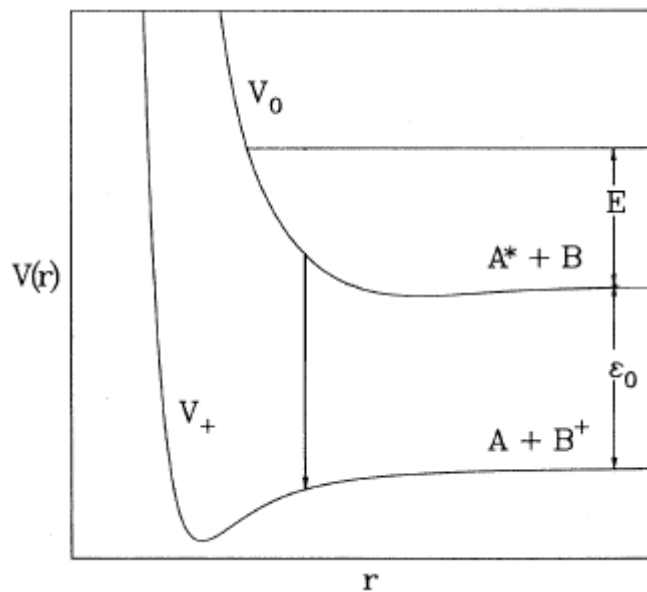


Figure 7: Transition between V_0 and V_+ .

The effect is clearly illustrated in Figure 6. The centrifugal barrier is such that for high enough impact parameters the molecules will not come close enough to undergo a reaction.

A bit should be said regarding impact parameters. It is not obvious for the hard sphere scattering case that the impact parameter often depends on the kinetic energy of the incident object.¹⁸ The incident molecule's kinetic energy will affect the so-called differential cross section, D . D is a ratio of cross section differential ($d\sigma$) and the solid angle differential ($d\Omega$) – see the scattering Figure 5 for clarification. D depends on the scattering angle and the impact parameter, though the exact dependence varies between systems. However, the total collision cross section, σ , is just the integral of D over $d\Omega$. This means that the collision cross section depends on the impact parameter b . The larger the collision cross section the more reactions occur and the more electrons are ejected during a Penning Ionization reaction. Thus the impact parameter (incident molecule kinetic energy) has a direct effect on the populations observed for electron spectra. It is useful to observe this dependence by running similar experiments at varying kinetic energies.

We now know that the impact parameter is a measure of the nearness of a collision. We will see in the next section that the reaction will occur at a variety of impact parameters due to the uncertainty of quantum mechanics. It is also important to discuss what effect the total energy of the system will have on the ejected electrons' kinetic energies. This will be covered in the next section.

¹⁸ *Introduction to Quantum Mechanics*; David Griffiths; Pearson Prentice Hall; 2nd Ed.; 2004; page 397

Two Potential Model

Penning Ionization reactions involve the rearrangement of electron configurations. The reaction is best thought of as a vertical jump between two potential energy curves, one curve for the reactants and one curve for the products. Refer to Figure 7 for an example. This two potential model describes the potential energy of $A^* + B$ as a function $V_0(R)$ and the potential energy of $A + B^+$ as a function $V_+(R)$. A reaction of $A^* + B \rightarrow A + B^+ + e^-$ is described as a vertical jump¹⁹ between the two potential energy functions. The difference between V_0 and V_+ when the reactants are infinitely far apart is ϵ_0 . ϵ_0 is determined by the relation:

$$\epsilon_0 = E(A^*) - IP(B) \quad (10)$$

where $E(A^*)$ is the excitation energy of A^* and $IP(B)$ is the ionization potential of B .

The excitation energy of A is the amount of energy needed to promote A to the A^* metastable state. The ionization potential of B is the amount of energy needed to remove an electron from an orbital – this will differ based on the orbital from which the electron is removed. If the reaction occurred when the molecules were infinitely far apart then this would be the kinetic energy of the ejected electron.

In reality the reaction will occur when the molecules are close to each other, not an infinite distance away from each other. If this were a classical phenomenon things would be much simpler; the reactants would react upon collision. However, a purely classical theory is insufficient to explain observed data. A classical explanation would predict a very narrow peak width. A narrow width would arise when the reaction only takes place over a small range of r values (and a small range of impact parameters. To

¹⁹PENNING IONIZATION OF SMALL MOLECULES BY METASTABLE NEON, Univ. Pitt, Thesis, Joe Noroski, 2007, page 8.

properly explain how this system reacts we need to introduce a resonance width, $\Gamma(R)/2$. The meaning of the resonance width is explained in more detail in Appendix A2. For now, it will suffice to say that the resonance width determines the probability that a reaction will occur at a given distance, r . See Figure 8 for a plot of the resonance width along side of the two potential model. The resonance width expresses the probabilistic nature of the Penning Ionization reaction. In some instances the reaction will occur at a closer distance than is expected and in other instances the reaction will occur at a further distance than is expected.

Now let's look at the dependence of the potentials on the intermolecular distance r . Now we have $V_0(r)$ and $V_+(r)$. Both $V_0(r)$ and $V_+(r)$ follow the Morse potential model – although $V_0(r)$ can be very shallow. The difference between these two functions is $\epsilon(r)$, which is now based on ϵ_0 and the forces between reactants. We can also define a kinetic energy function, $E(r)$, which is the difference between the total energy of the system, E_{tot} , and the potential energy, $V_0(r)$. The total energy of the system before a reaction can be described by:

$$E_{\text{tot}} = E(r) + V_0(r) \quad (11)$$

After a reaction the potential undergoes a vertical jump and the potential energy function changes from $V_0(r)$ to $V_+(r)$. The total energy of the system is now expressed:

$$E_{\text{tot}} = E'(r) + \epsilon(r) + V_+(r) \quad (12)$$

where $E'(r)$ is the kinetic energy of the products.

We now see the kinetic energy of the ejected electron is dependent on the intermolecular distance r . Due to the attractive and then repulsive nature of the potential curve $V_0(r)$ there exists an intermolecular distance where the repulsive and attractive

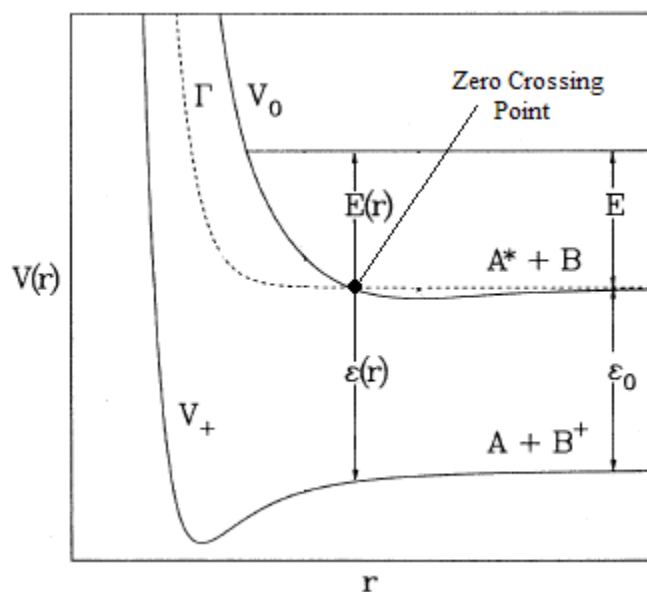


Figure 8: Illustration of the zero crossing point. An imaginary potential Γ is added in order to account for the probability of reaction. This is described in detail in Appendix A2.

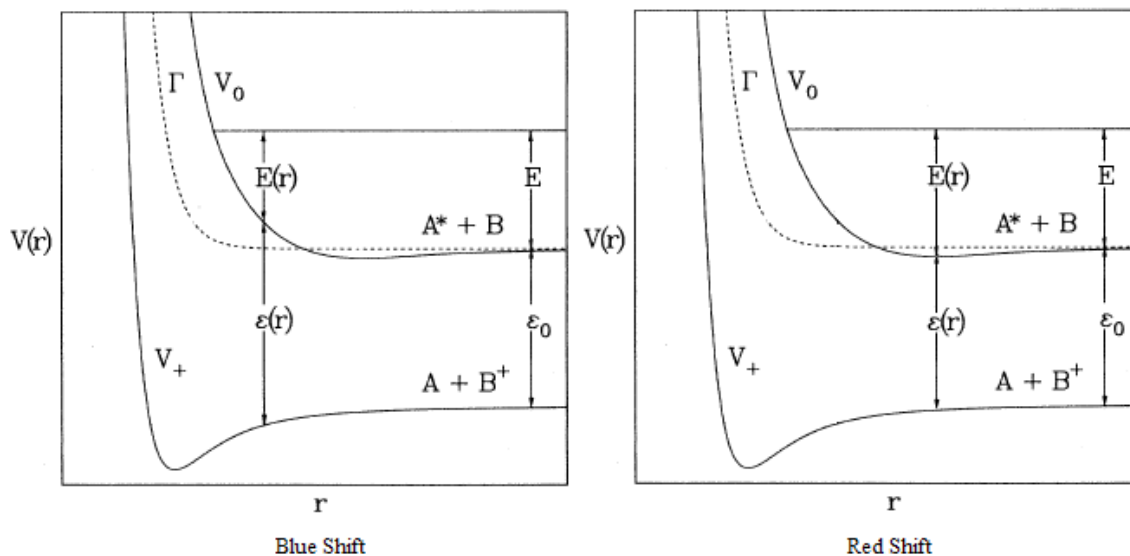


Figure 9: The reaction is indicated by the vertical line. For a blue shift the reaction occurs to the right of the zero crossing point and for a red shift the reaction occurs to the left of the zero crossing point.

molecular forces cancel one another; let's call this distance r_0 . This point is called the zero crossing point (when a potential curve changes sign) and is the point on the function $\epsilon(r_i)$ where $\epsilon(r_0) = \epsilon_0$.²⁰ The zero crossing point is illustrated in Figure 8. If the reaction occurs at the zero crossing point the ejected kinetic energy is equal to $\epsilon_0 = E(A^*) - IP(B)$, just as if the reaction had occurred at infinite separation. Stated in another way, the zero crossing point is a point on $V_o(r)$ where the reaction will occur as though no forces act on the reagents.

However, the resonance width tells us that the reaction will not always occur at ϵ_0 . In fact the reaction often occurs over a range of impact parameters and intermolecular distances due to the probabilistic nature of the reaction. If the reaction occurs at a distance where $r < r_0$ then the observed electron kinetic energy will be greater than ϵ_0 and we call the electron blue shifted. Conversely, if the reaction occurs at a distance where $r > r_0$ then the observed electron kinetic energy will be lesser than ϵ_0 and the electron is red shifted. The spread in electron kinetic energies around ϵ_0 is due to the uncertainty in the r value for which the reaction occurs.

Let's look at what happens in the event of a blue shift. In this case the reaction will occur when the r is in the repulsive portion of the potential, $V_o(r)$. A reaction at this position of r will produce an $\epsilon(r_0) > \epsilon_0$. Similarly, in the event of a red shift the reaction will occur in the attractive region of the potential, $V_o(r)$. This reaction produces an $\epsilon(r_0) < \epsilon_0$. Refer to Figure 9 for an illustration of this. Both blue and red shifts will occur during the course of many reactions. However, looking at Figure 8 it is apparent that the resonance width is larger at distances where $V_o(r)$ is repulsive. This suggests that we will

²⁰ PENNING IONIZATION OF SMALL MOLECULES BY METASTABLE NEON, Thesis, Joe Noroski, 2007, page 8

see more reactions occurring a while the molecules experience repulsive forces. This is not always true and could change depending on the molecules used in the reaction; for this research this will turn out to be the case.

It is, however, incorrect to think that the red or blue shift is dependent only on the force between the two reagents. There is also a dependence on the total energy of the system.²¹ The dependence on total energy manifests itself in $V_0(r)$ in a manner described by Figure 6. $V_0(r)$ is in fact the effective potential and has the centrifugal energy term built in to it; thus $V_0(r)$ should increase with increasing E_{tot} . The blue and red shifts' dependence on total energy can be measured by observing the kinetic energies of the ejected electron over a range of initial total energies. In this way we can determine the shape of the initial V_0 curve up until the transition to V_+ occurs for a specific system total energy.²²

²¹ *PENNING IONIZATION OF SMALL MOLECULES BY METASTABLE NEON*, Univ. Pitt ,Thesis, Joe Noroski, 2007, page 9.

²² *PENNING IONIZATION OF SMALL MOLECULES BY METASTABLE NEON*, Univ. Pitt ,Thesis, Joe Noroski, 2007, page 9.

Potential Energy Surfaces

A potential energy surface contains – when used in conjunction with the Hamiltonian and the Schrödinger equation – all of the dynamical information about a chemical reaction. Obtaining a potential energy surface of a Penning Ionization reaction is a great step forward in understanding the reaction. Unfortunately, potential energy surfaces for molecular collisions can be difficult to obtain, especially for a polyatomic molecule. It is indeed difficult to map the entire potential surface; however, we can still obtain information regarding the key features – hills and valleys - of the potential energy surface.

Before going any further it is necessary to distinguish between two ways to approach the topic of potential energy surfaces. The first way is more thorough and involves considering the potential between each atom or approach angle. For the simplest case we have the familiar Morse potential. Two spherically symmetric atoms approach each other due to an attractive force between them ($V < 0$). At certain point in their approach the atoms will begin to feel the repulsive force and be driven apart. Typically there is a minimum potential where the atoms are in the most stable configuration.

Suppose that one of the atoms in the previous discussion was not spherically symmetric (let us allow azimuthal symmetry). The potential energy curve based only on inter-nuclear distance is no longer enough to describe the interaction. We need to find the potential curve for all approach angles, 0 to 2π . The result is a potential energy surface that depends on two reaction coordinates. The reaction coordinates in this case are the inter-nuclear distance, r , and approach angle, θ . It is easy to see how adding

nuclei and asymmetry will quickly increase the number of reaction coordinates needed to describe the molecular interaction. These reaction coordinate hypersurfaces can be displayed by using many contour plots.

Alternately, we can consider making an intermolecular potential energy surface between the incoming atom and the target molecule while keeping the molecular degrees of freedom frozen. This keeps the surface in the third dimension but does come at the cost of exactness. This approximation is justified by the Franck-Condon approximation because for the electronic transition the nuclei are essentially frozen out anyway. The potential energy surface is now a function of reaction coordinates r and θ , intermolecular distance and approach angle respectively.²³ Now the question is how will we be able to construct an intermolecular potential energy surface from the crossed beam experiment?

The electrons ejected from the Penning Ionization reaction can only give us information about the collision between the two reagents. No information can be obtained about long range features of the PES. However, from the Penning Ionization electron spectrum we can learn about the repulsive or attractive forces between the two reagents as they approach each other. In this way, the Penning electron can tell us about the key features of the potential energy surface.

The key to gaining information about the features of a potential energy surface is the resonance width, $\Gamma(r)$. From Miller's review article^{24,25} it is shown that the following relation exists between the resonance width and the reactant potential:

$$\Gamma(r) = 2\pi\rho_e|V_{oe}(r)|^2 \quad (13)$$

²³ *Quantum Chemistry and Spectroscopy*; Thomas Engel; Pearson Education; 2006; page 325.

²⁴ *Computation of Auto-Ionization Life Times via a Golden Rule*; W. H. Miller; Chem. Phys Letters.; Issue 4 Page 627; 1970

²⁵ *Theory of Penning Ionization*; W. H. Miller; J. Chem. Phys.; Vol 52; Number 7; 1970

where ρ_ϵ is the density of states (units of eV^{-1}) and $|V_{0\epsilon}|^2$ is the square of the magnitude of the matrix element. The matrix element is described by equation 14.

$$V_{0\epsilon}(\mathbf{r}) = \langle \psi_0 | H - E(\mathbf{r}) | \psi_+ \rangle^{26} \quad (14)$$

From equations 13 and 14 it is apparent that the resonance width depends on the expectation value of $V_0(\mathbf{r})$. This correlation between resonance width and reactant potential is useful as we can safely make a prediction about where the activation energy peak on the reaction path will occur – the reaction will occur when the repulsive force between reactants is dominant. This is the information regarding potential energy surfaces that can be obtained from a PIES experiment; note that no information can be obtained regarding the outgoing potential energy surface of the products. We can compare experimental data with theory to gain a crisper picture of a particular intermolecular PES. For example, we can model an intermolecular PES using a computer program such as Gaussian. The two key features of a PES are the hills and valleys. The hills are representative of the activation energy reactants must overcome in order for the reaction to occur.

For a potential energy surface as a function reaction coordinates (i.e. reagent \rightarrow transition state \rightarrow product) the position of the hill along the reaction coordinates depends on whether the reactants repel or attract one another. If the reactants attract one another then the hill will appear earlier along the reaction path; energy will be released as the reactants are brought closer to one another. If the reactants repel one another then the hill will appear later along the reaction path; energy will be released as the reactants move

²⁶ *Computation of Auto-Ionization Life Times via a Golden Rule*; W. H. Miller; Chem. Phys Letters.; Issue 4 Page 627; 1970

further away.²⁷ It is now possible to map a feature of the Penning electron – kinetic energy – to a feature of the intermolecular PES – relative position of activation barriers. This is shown in Figure 10. However, the Penning Ionization reaction is not as gradual as Figure 10 suggests. The emission of an electron is a highly irreversible step that results in a decrease of the system's overall total energy. A more realistic potential energy curve is shown in Figure 11. Here the transition is not a gradual hill but, rather, a steep cliff. There is still a distinction between attractive and repulsive forces. If the forces between the molecules is repulsive there will be a hill leading up to the cliff whereas for a attractive forces there is downward slope before the cliff. This distinction is the sort of qualitative information that we can learn about potential energy surfaces from PIES.

Similarly, in order to make qualitative inferences about the intermolecular potential energy surface we need to know if the measured Penning electrons are gaining kinetic energy or losing kinetic energy. To do this we need to compare the observed electron kinetic energies to the expected kinetic energies based on the difference between the excitation energy of A and the ionization energy of B, ϵ_0 . If the majority of observed electron kinetic energies are greater than ϵ_0 (blue shifted) then the force between the molecules is likely to be repulsive. Likewise, if the electron kinetic energies are less than ϵ_0 then the force between the molecules is likely attractive. The respective PES hill properties can thus be inferred.

The blue and red shifts are the key feature of the electron spectrum for making qualitative statements about the intermolecular potential energy surface. If the spectrum is blue shifted then this will suggest that the resonance width is greatest at the repulsive part of the potential. It will suggest further that the force between the reactants was

²⁷ *Chemical Kinetics and Reaction Dynamics*, Upadhyay. Page 220

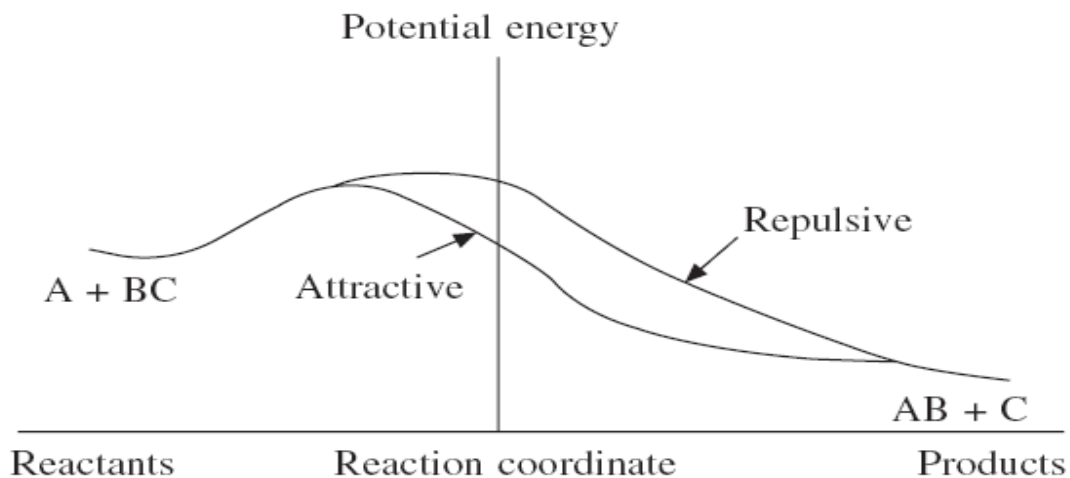


Figure 10: The difference in hill position for attractive and repulsive forces for a typical reaction.²⁸

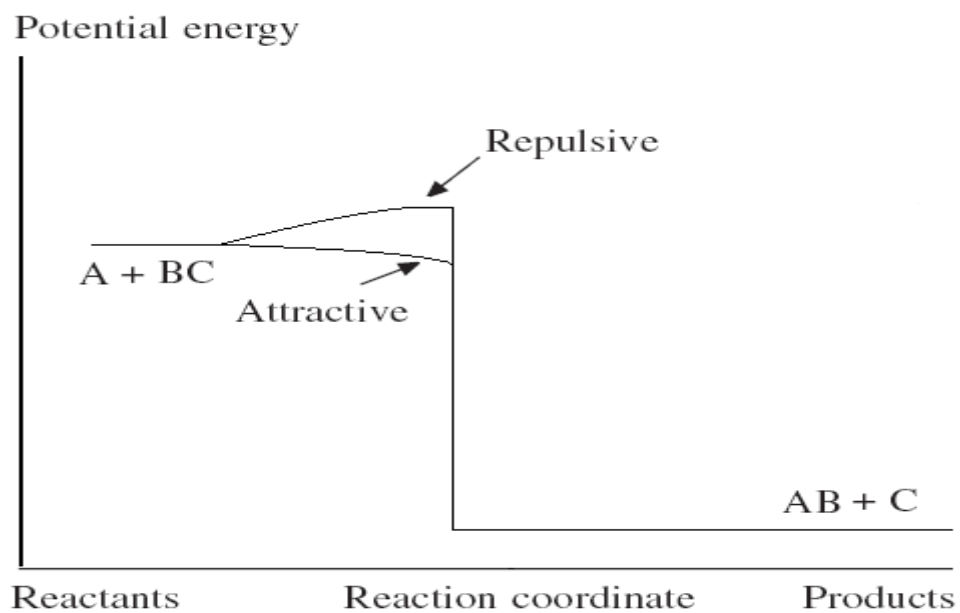


Figure 11: This is the potential energy curve for the Penning Ionization reaction. A is Ne^* and BC is N_2O . After the reaction, C would be the electron and AB is an NeN_2O^+ complex just before dissociation.

²⁸ *Chemical Kinetics and Reaction Dynamics*, Upadhyay. Page 231

Similarly, a red shift would suggest that reaction occurred when the forces between the reactants were attractive. In this way we can determine whether there is a hill or a valley on the intermolecular potential energy surface at the point (or rather range) of reaction.

Experimental

Overview

Electron spectra of pure Penning Ionization reactions between Ne^* and N_2O are obtained at initial collision energies (E_{tot}) of 0.075eV/mol and 0.136eV/mol. For the purposes of calibration, Ne^* , $\text{HeI} + \text{N}_2\text{O}$ electron spectra were obtained at initial collision energies of 0.075eV/mol and 0.136eV/mol. A pure $\text{HeI} + \text{N}_2\text{O}$ electron spectrum was taken as well for purposes of calibration. The Ne^* was introduced to the main chamber via the primary beam source and N_2O was introduced - at a 90° angle from the primary beam source - via the secondary beam source. HeI photons were provided from a UV-lamp that is at a 90° angle with respect to the secondary beam source and runs anti-parallel to the primary beam source (see Figure 12). For a list of the equipment used refer to Appendix A-4.

Supersonic Beams

Supersonic molecular beams are used for production of both primary and secondary molecular beams. Molecules prepared in this manner are forced from a concentrated area to a more dilute area, resulting in a temperature drop. This cooling effectively eliminates rotational and vibrational excited states via the Joule-Thomson Effect.²⁹ This is useful for our purposes as fewer vibrational states will simplify the spectrum considerably; in fact the cooling removes most of the energy out of the rotational and vibrational degrees of freedom. Furthermore supersonic beams also produce a narrow velocity distribution. This will be valuable in obtaining narrow electron kinetic energy distributions. A third

²⁹ *Principles of Thermodynamics*; George Alfred Goodenough; Holt; 1911; page 276

advantage to this production method is the

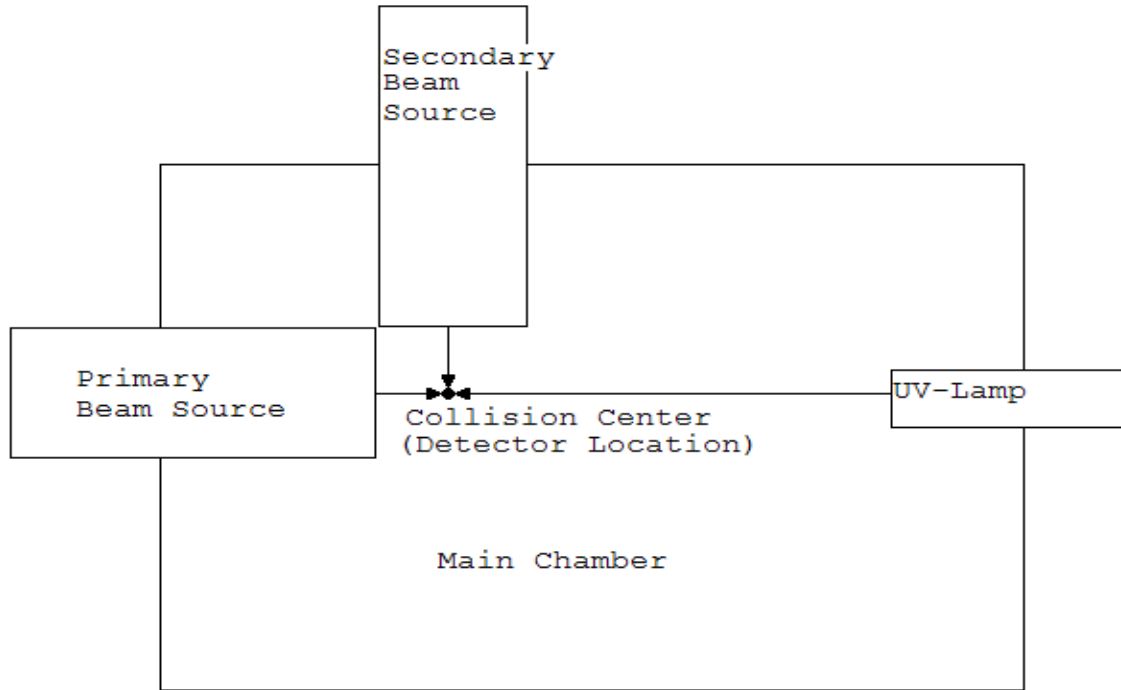


Figure 12: The general setup of the main chamber and beam sources.

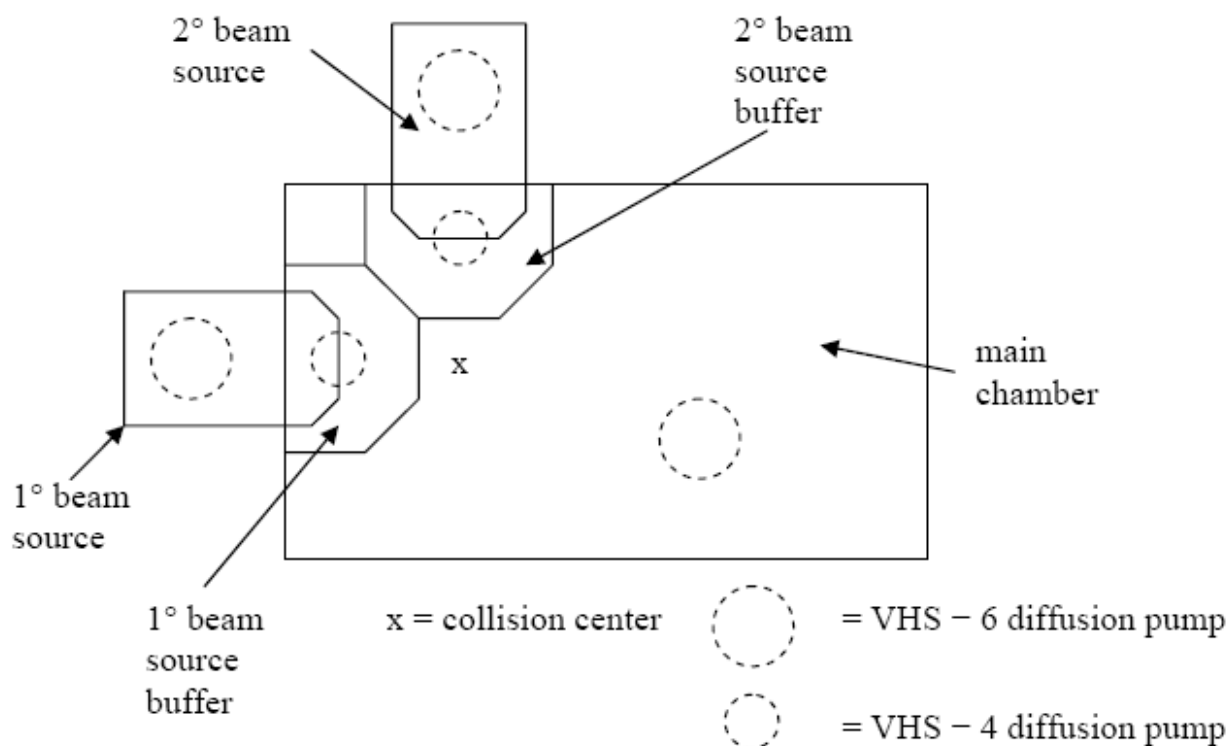


Figure 13: The location of the diffusion pumps for the vacuum system.³⁰

fact that the supersonic beams produce a large population of molecules traveling in the desired direction; this results in a more reactions and thus a more intense signal.³¹

Preparation of Reagent's Internal Energy

If we are going to observe the magnitude of red/blue shift as a function of initial total system energy we need to make sure we prepare our states correctly. If we fail to account for some degrees of freedom our correlation of temperature to energy could be incorrect. Due to the use of supersonic nozzles (discussed above) most of the energy has been removed from the rotational and vibrational degrees of freedom. With the internal energy

³⁰ PENNING IONIZATION OF SMALL MOLECULES BY METASTABLE NEON, Thesis, Joe Noroski, 2007, page 14

³¹ PENNING IONIZATION OF SMALL MOLECULES BY METASTABLE NEON, Thesis, Joe Noroski, 2007, page 16

dependent only (or very nearly) on the translational motion of the molecule it is possible to correlate temperature and the total energy of the reagent system easily.

The temperature of the reactants is controlled by the nozzle of the beam source. Specifically, the temperature of the nozzle is controlled by an applied voltage. The temperature of the nozzle determines the initial collision energy of the reactants in a rather complicated manner. We start with the relation of the energy of the system and the molecules' average velocities given by:

$$E = \frac{1}{2} \cdot \mu \cdot \left[\left(v(\text{Ne})_{\text{mp}} \right)^2 + \left(v(\text{N}_2\text{O})_{\text{mp}} \right)^2 \right] \quad (15)$$

where $v(\text{molecule})_{\text{mp}}$ is the most probable velocity of that molecule and μ is the reduced mass of the system. The most probable velocity most likely velocity for any molecule in the system to have; it is the maximum value of the velocity distribution. The most probable velocities are given by equation 16:

$$v_{\text{mp}} = \sqrt{\frac{\gamma}{\gamma - 1}} \cdot \sqrt{\frac{2k \cdot (T_0 - T)}{m}} \cdot \left[1 + \frac{1}{\left(\frac{M^2 \cdot \gamma}{2} \right)} \right] \quad (16)$$

where M is the mach number, T_0 is the nozzle temperature, T is cooled translational temperature, m is the molecular mass, k is the Boltzmann constant, and γ is the ratio of C_p/C_v . This formula will give the most probable velocity for each molecule type at a given nozzle temperature. To calculate the cooled translational temperature we use the following formula:

$$T = \frac{T_0}{1 + M \cdot \frac{(\gamma - 1)}{2}} \quad (17)$$

which relates T to the mach number and the nozzle temperature. This description is a bit condensed and avoids most of the theory behind arriving at this result.³²

Typical mach numbers for Ne^* and N_2O are 15 and 8.4 respectively. γ has value of $5/3$ for Ne^* and $7/5$ for N_2O (and other linear polyatomic molecules).

Production of Ne^* and Electron Gun

Ne^* is produced by bombarding Ne with an electron gun (described below). After selection rules are considered, there are only two metastable excited states for Ne^* - the $^3\text{P}_2$ and $^3\text{P}_0$ states. These two states have a difference in energy due to the difference in j values.^{33,34} This will produce a slight separation of peaks in the final spectrum.

The electron gun used in the production of Ne^* metastables is illustrated in Figure 14. The circuit diagram for the electron gun is shown in Figure 15. The electrons are generated from a heated tungsten filament via thermionic emission; the filament is kept at a -400V bias with an emission current of around $1/3\text{A}$. Once the electrons are generated they react with the Ne creating Ne^* or Ne^+ . The grounded tungsten mesh between the upstream deflector and the filament serves to direct the electrons emitted from the filament. Pinch electrodes, downstream of the filament, are held at a -600V bias to focus electrons toward the electron gun center.³⁵

We need a way of allowing only Ne^* to pass through the gun, this is accomplished by two deflectors - upstream and downstream. The deflectors are kept at a

³² PENNING IONIZATION OF SMALL MOLECULES BY METASTABLE NEON, Thesis, Joe Noroski, 2007, page 43

³³ PENNING IONIZATION OF SMALL MOLECULES BY METASTABLE NEON, Thesis, Joe Noroski, 2007, page 17.

³⁴ *Magnetic Deflection Analysis of Supersonic Metastable Atom Beams*; Weisner and Siska; 1987; Rev. Sci. Instruments; 58; page 2124

³⁵ *The Collision Dependence of Penning Ionization of Nitrogen Molecules by Metastable helium as Determined by Electron Spectroscopy*; Dunlavy; PhD. Thesis; University of Pittsburgh; 1996; page 34

bias of -600V (sometimes -550V). The upstream deflector will prevent Ne^+ ions and electrons from passing backwards into the skimmer; whereas the downstream deflector prevents Ne^+ ions and electrons from becoming part of the collimated beam. In this way only the neutral Ne^* atoms are allowed to become part of the molecular beam; anything with a charge is filtered out.

A bit should be said about the preparation of the metastable states of Ne^* . Using the electron gun to create excited states of Ne is not very selective and will produce the $^1\text{P}_1$, $^3\text{P}_0$, $^3\text{P}_1$, and $^3\text{P}_2$ states. If all of these states made it into the beam, the result would be a very messy spectrum. Selection rules (i.e. rules governing what transitions can take place) will eliminate the $J = 1$ states from the beam. The relevant selection rules for a transition are $\Delta J = 0$ or ± 1 , $\Delta L = 0$ or ± 1 , and $\Delta S = 0$. These rules allow for the $^1\text{P}_1$ and $^3\text{P}_1$ states to relax to the ground state ($^1\text{S}_0$). However, for the $^3\text{P}_0$ to relax due to the rule $\Delta S = 0$; there will not be a sudden transition from triplet to singlet states. As a result of these rules the singlet states will relax. The relaxation is electronic and thus the relaxation occurs much faster than the Ne nuclei move. Because of this, the singlet states will relax well before entering the main chamber leaving only the metastable triplet states.

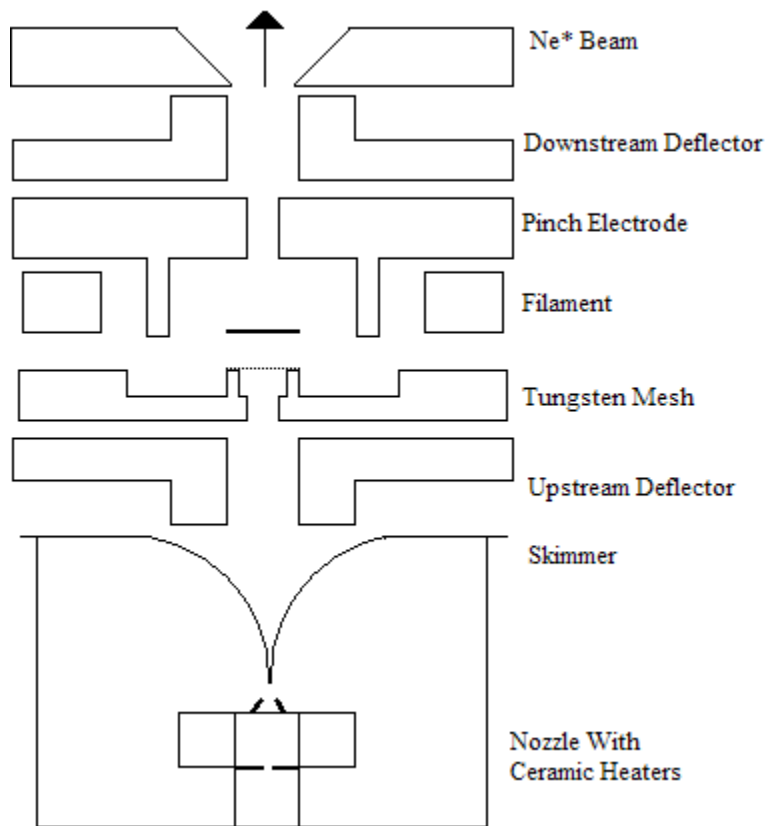


Figure 14: Schematic of the electron gun.

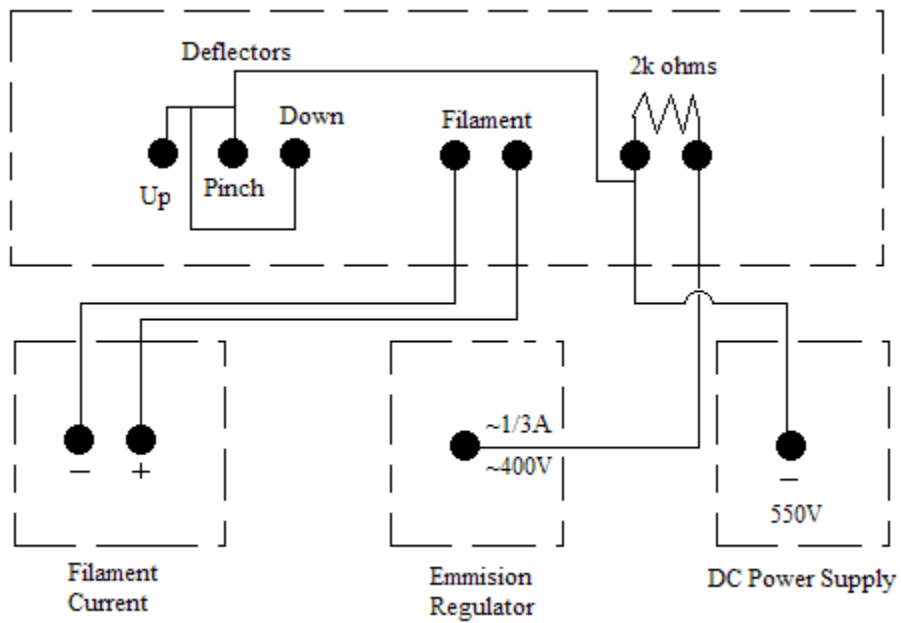


Figure 15: Circuit diagram for the electron gun.

Vacuum System and Main Chamber

The reaction takes place in the main chamber. This hollow, aluminum, cubic chamber has interior dimensions $32\frac{1}{4}'' \times 31'' \times 24''$. The chamber has a Helmholtz coil on each side in order to minimize effects of stray magnetic fields on the reaction center. There are two beam sources which plug into adjacent sides of the chamber (see Figure 12). The metastable beam will be introduced by the primary beam source and the target molecule will be introduced via the secondary beam source. The two sources are kept at a 90° angle from each other. Opposite the primary beam chamber is a Helium beam source and UV-lamp - this will be used to run the calibration spectra using HeI.

It is often necessary to vent one part of the chamber while keeping the other parts under vacuum. For this reason the primary and secondary beam sources have their own mechanical/diffusion pump system. Gate valves separate the diffusion pump from respective chamber – a diagram of the vacuum system for this machine is provided (Figure 13). Typically, experiments are performed at a pressure of about 5×10^{-6} torr in the main chamber. This pressure is observed via an ion gauge on each chamber.

Electron Analyzer

The electron analyzer is typical of an electron spectrometer. It contains three essential parts. The first part is the Einzel lens; this is where the electrons are focused after entering the analyzer. The Einzel lens focuses electrons – or any ion – in much the same manner a lens can be used to focus light (see Figure 16). The Einzel lens consists of three plates: two outer plates and an inner plate that is sandwiched between the two outer plates. The inner plate is kept at higher voltage than the grounded outer plates; this is

illustrated in the Einzel lens' circuit diagram, Figure 17. The Einzel lens also serves as a means of selecting which kinetic energy electrons we wish to observe. If an electron has a too high or low a kinetic energy then the electric field will send the electron into one of the grounded outer plates. By controlling the voltage of the inner lens it is possible to select what range of electron kinetic energies we wish to observe. The outer lenses are set to 0.012V while the inner lens is set to 0.020V. The image below demonstrates how the electric field lines will focus the incident electrons.

The second is portion of the analyzer is the hemispherical field (see Figure 18). This is where we select which electrons we would like to look at. There is a magnet at the center of this hemispherical portion. The magnet causes incoming electrons to curve

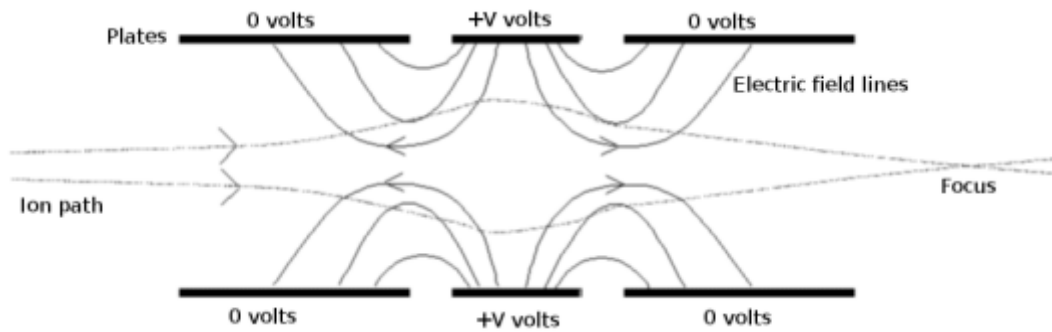


Figure 16: An illustration of how an Einzel lens works to focus electrons. The inner and outer lenses are kept at different voltages which focus the electrons just as an optical lens focuses photons.³⁶

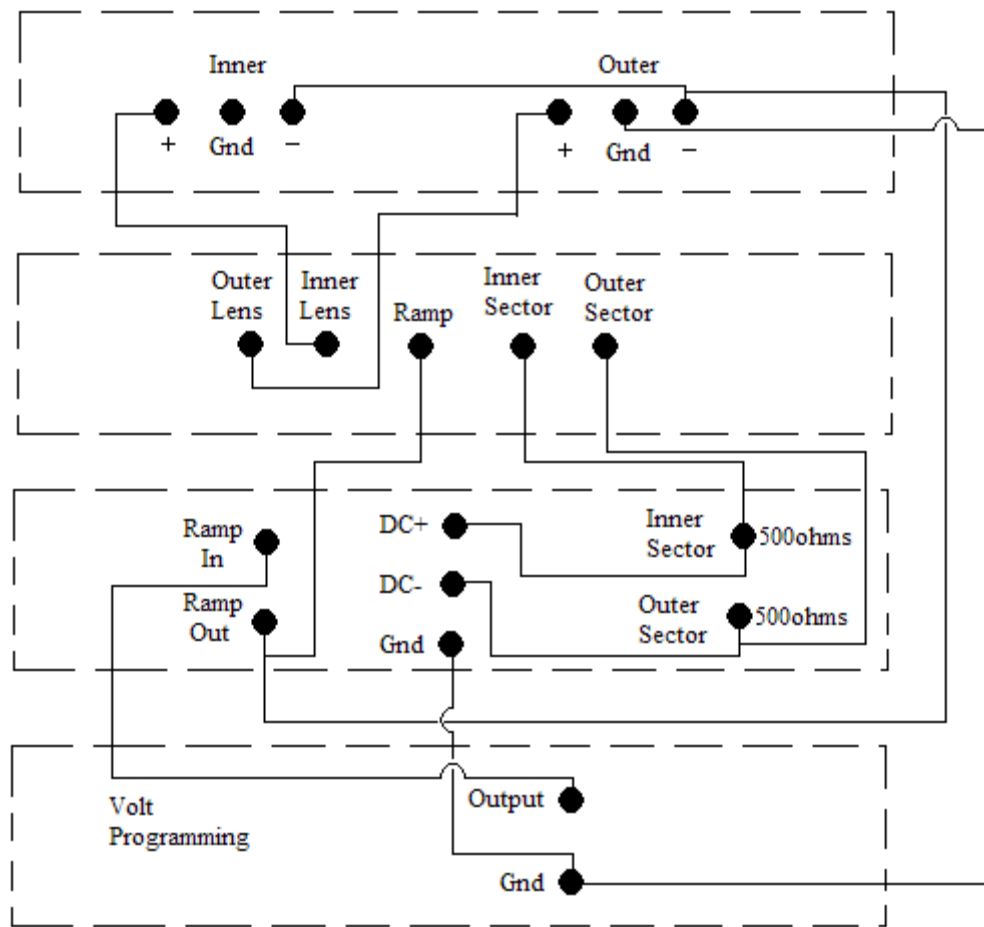


Figure 17: Circuit diagram for the Einzel lens and related electronics.

³⁶ Image from http://en.wikipedia.org/wiki/Image:Einzel_lens.png

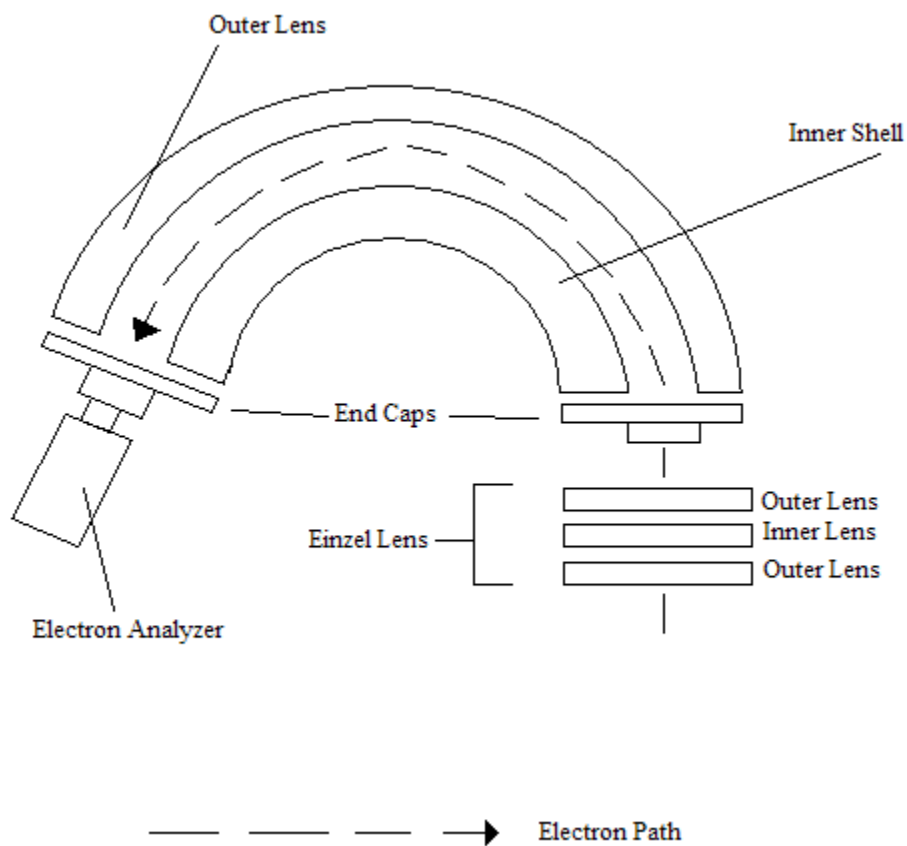


Figure 18: Rough diagram of the electron analyzer.

using the Lorentz force law - $F = q(E + v \times B)$. Because of the magnet the electrons will curve while in the analyzer's hemispherical piece. The hemisphere also serves as another means of selecting only electrons with the appropriate kinetic energy will be curved enough to reach the analyzer - the others will hit the walls of hemispherical piece. The walls of the hemispherical piece are coated with graphite in order to absorb stray electrons.

I would like to digress a bit in order to discuss the pass energy of the analyzer. The circuit for the analyzer system suggests that the pass energy will be related to the radii of the sectors by:

$$E_{\text{pass}} = \frac{\Delta V}{\left(\frac{r_1}{r_2} - \frac{r_2}{r_1} \right)} \quad (18)$$

where ΔV is the potential difference between the inner and outer sectors, r_1 is the radius of the outer sector (4.05cm) and r_2 is radius of the inner sector (3.25cm); this gives $E_{\text{pass}} = 2.254 \Delta V$. In order to filter through a range of pass energies we have to increase the ramping voltage through a range of voltages. The ramping voltage and the pass voltage are related as shown by:

$$E_{\text{pass}} = V_{\text{ramp}} + E_e \quad (19)$$

where E_e is the electron kinetic energy.³⁷ By maintaining E_{pass} at a constant value (3.5V) and varying the ramp voltage we can make the analyzer respond to a range of electron kinetic energies (one at a time of course). The virtue of the constant pass energy set up is

³⁷ *The Collision Dependence of Penning Ionization of Nitrogen Molecules by Metastable Helium as Determined by Electron Spectroscopy*; Dunlavy; PhD. Thesis; University of Pittsburgh; 1996; page 37

that the analyzer always detects electrons of the same energy. This allows for a consistent resolution to be obtained over a range of kinetic energies – other setups could result in a resolution that varies with electron kinetic energy.

The third part of the analyzer is the transducer. This is a standard electron multiplier. This detects the few electrons that make it through the hemispherical piece; it then multiplies the signal and sends it to a counter. A computer is used to run through a range of voltages and display the average count for each. After about forty runs - giving a signal to noise ratio of about 6.3 - through the voltages, we should have a usable spectrum.

Data Analysis

The reaction $\text{Ne}^* + \text{N}_2\text{O}$ was run at collision energies of 0.075eV and 0.136eV. This corresponds to Ne^* nozzle temperatures of 40°C and 450°C respectively (as described in the experimental section).

Calibration

To calibrate the spectrum we need to look at the expected peak positions of the Ne^* , HeI + N_2O spectrum.³⁸ The expected peak positions (for the photoelectric peaks) are obtained by subtracting the adiabatic ionization potentials of N_2O (see Table 1) from the transition energy of the HeI radiation (21.21804eV). The average discrepancy between the expected peaks and the observed peaks are used to shift the peaks to their appropriate positions. The expected HeI peak positions for the X, A, and B states of N_2O are 8.29eV, 4.79eV, and 3.52eV respectively. Figure 19 and Figure 20 show the Ne^* , HeI + N_2O spectra at collision energies of 0.075eV and 0.136eV respectively. Both spectra place the A state peak at 4.56eV. This results in an average shift of 0.23eV. This shift will be added to the electron kinetic energy for the PIES spectra in order to bring the PIES peaks to their correct positions.

Raw PIES Transmission Correction

The first step in the data analysis is to correct for the Einzel lens. The Einzel lens is better at accepting lower energy electrons than higher energy electrons, thus peak intensities of the raw spectrum are not accurate. To correct for this a FORTRAN

³⁸ *Handbook of HeI Photoelectron Spectra of Fundamental Organic Molecules*; K. Kimura, S. Katsumata, Y. Achiba, T. Yamazaki, S. Iwata; Halsted Press, New York; 1981

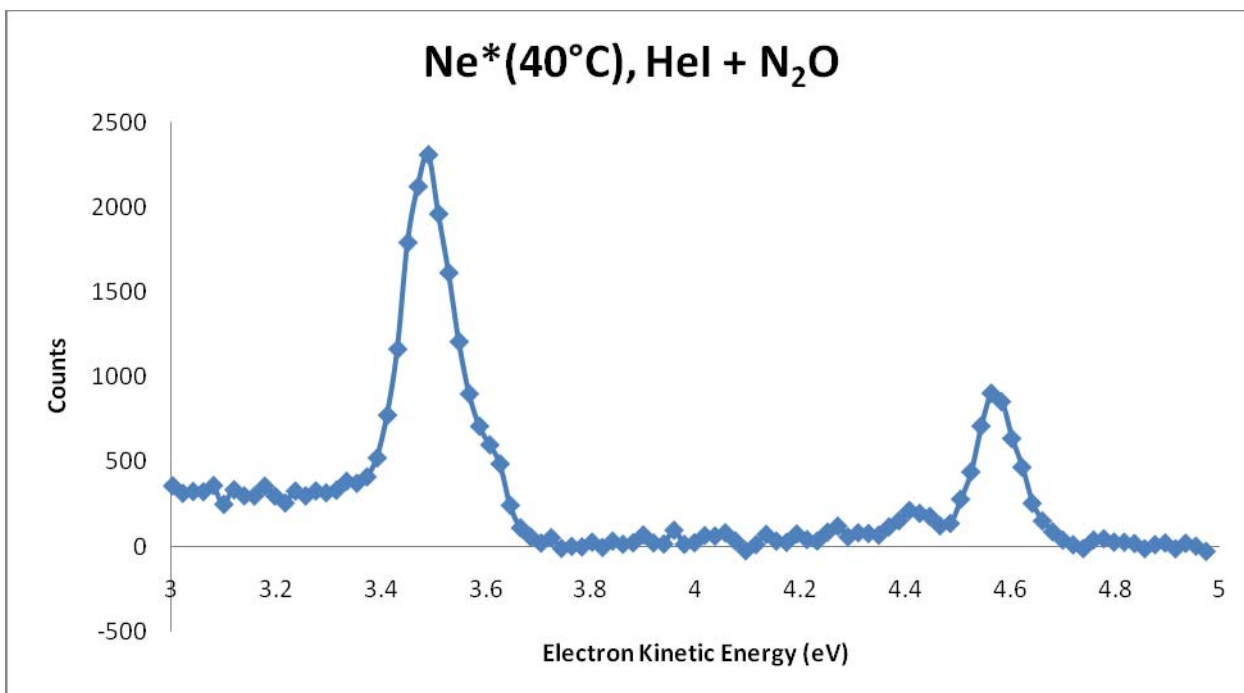


Figure 19: HeI calibration spectrum with the Ne* + N₂O reaction with a collision energy of 0.075eV. The HeI peak is located at 4.56eV.

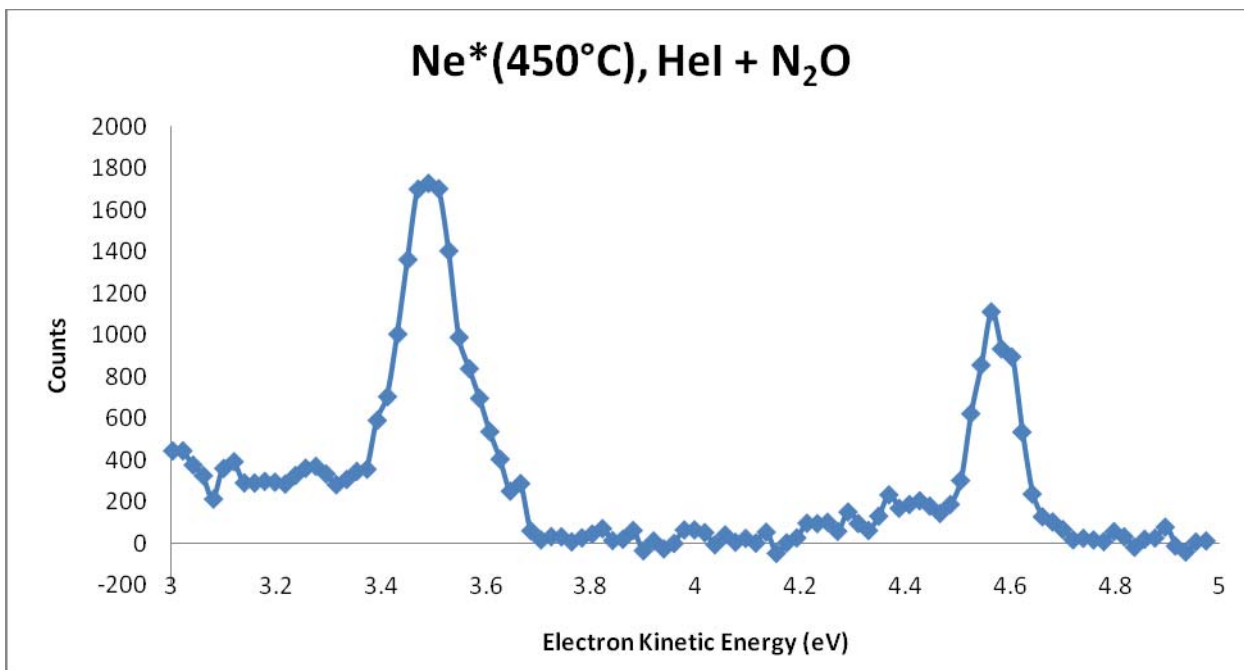


Figure 20: HeI calibration spectrum with the Ne* + N₂O reaction with a collision energy of 0.136eV. The HeI peak is located at 4.56eV.

program written by P. E. Siska is used. This is admittedly a bit of a black box in this thesis. The transmission corrected and shifted spectra are shown in Figure 21 and Figure 22.

Peak Shifts

Looking at the PIES spectra (Figure 21 and 22) we see three major peaks. The peak at about 0.95eV is of unknown origin as it does not correspond to any kinetic energy values we would expect based on differences between the excitation energy of Ne* and adiabatic ionization energies of N₂O. Using Table 1 (the adiabatic ionization energies for N₂O and Table 2 (the excitation energy for Ne*) we get an idea for where we expect to see peaks. Expected peaks values for the X and A state of N₂O are 3.73eV and 0.23eV respectively. The X state peak at 3.73eV and an A state peak at 0.23eV are due to Ne*(2p⁵3s³P₂). Similarly, Ne*(2p⁵3s³P₀) can ionize N₂O. Ne*(2p⁵3s³P₀) is less common than Ne*(2p⁵3s³P₂) and will result in X state and A state peaks of 3.83eV and 0.33eV respectively. These Ne*(2p⁵3s³P₀) peaks, however, are less intense and will overlap the more intense peaks due to Ne*(2p⁵3s³P₂); this will result in the shoulders on the observed peaks.

The observed peak for the A state occurs at an average energy of 0.27eV. This differs from the expected value (obtained from $\epsilon_0 = E(\text{Ne}^*(2p^5 3s^3 P_2)) - \text{IP}(\text{N}_2\text{O})$) of 0.23eV by a difference of 0.04eV. In this case $\epsilon(r_0) > \epsilon_0$ and indicates that the peak is blue shifted. The X state peak is observed to occur at an average energy of 3.74eV. The expected value is 3.73eV resulting in a difference of 0.01eV. Here, again, $\epsilon(r_0) > \epsilon_0$

shows that the peak is blue shifted. While the spectrum is undoubtedly blue shifted, it is

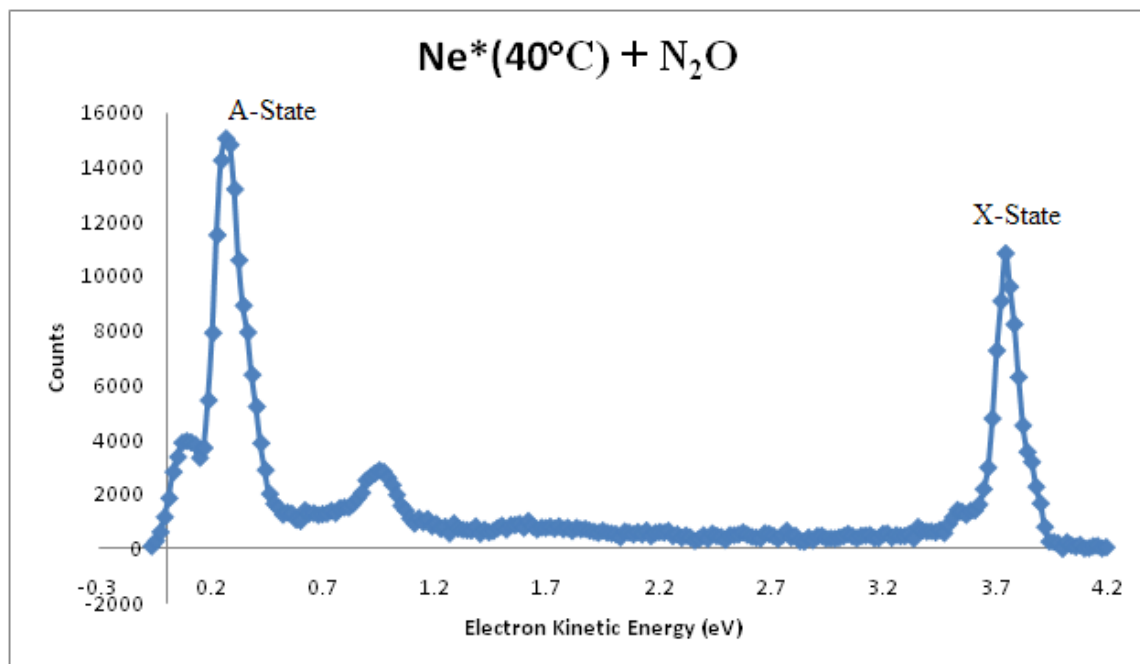


Figure 21: Ne* + N₂O PIES spectrum with a collision energy of 0.075eV. The X state is located at 3.74eV and the A state is located at 0.28eV.

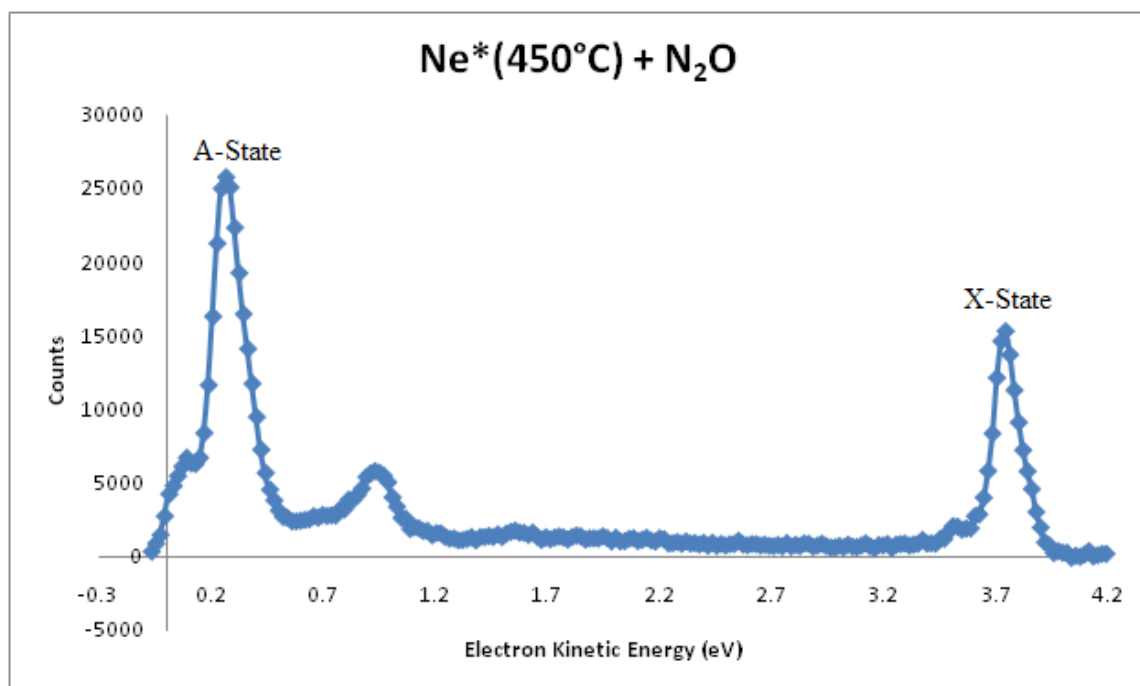


Figure 22: Ne* + N₂O PIES spectrum with a collision energy of 0.136eV. The X state is located at 3.74eV and the A state is located at 0.26eV.

| Atom | Electron Configuration | State | Excitation Energy (eV) |
|------|------------------------|----------|------------------------|
| He | $1s2s$ | 2^1S_0 | 20.6158 |
| | | 2^3S_1 | 19.8196 |
| Ne | $2p^53s$ | 3^3P_0 | 16.7154 |
| | | 3^3P_2 | 16.6191 |

Table 1: Excitation energies for He and Ne.

| Molecule | State | Adiabatic Ionization Potential (eV) |
|----------|-------|-------------------------------------|
| N_2O | X | 12.8898 |
| | A | 16.3896 |
| | B | 17.65 |
| | C | 20.11 |

Table 2: Adiabatic Ionization Potentials for N_2O ³⁹

³⁹ Tables 1 and 2 from *PENNING IONIZATION OF SMALL MOLECULES BY METASTABLE NEON*, Thesis, Joe Noroski, 2007, page 2, 24.

not blue shifted by a large amount.

Relative Populations

In order to obtain accurate information about the relative populations of the electronic states we need the area under each peak. The populations are dependent on the intensities of the peaks, the area under each peak. We need to fit the spectra to a curve in order to obtain accurate measures of the peak areas.

Fitting the spectrum is complicated by the fact that we are really looking at two spectra on top of one another: the 3P_2 and 3P_0 states of Ne*. However, looking at Figures 21 and 22 it is evident that the Ne*($2p^53s\ ^3P_0$) peaks are not resolvable. In fact, apart from a little shoulder on the A state peak there really is little evidence of the Ne*($2p^53s\ ^3P_0$) peaks. Unfortunately, this lack of distinguishable Ne*($2p^53s\ ^3P_0$) peaks will not permit any statements about the ratio of $^3P_2/^3P_0$ as it pertains to the Penning reaction.

One qualitative statement that can be made about the populations is with regards to the collision energies of the system. One spectrum was obtained with a collision energy of 0.075eV and the other with a collision energy of 0.136eV. Comparing Figures 21 and 22 we see a large increase in the intensity of the peaks. The A state peak is shown to have a height of about 15,000 counts at a collision energy of 0.075eV. For the spectrum with a collision energy of 0.136eV this same peaks has about 26,000 counts. This demonstrates that the collision cross section (which is reflective of the populations) increases with increasing collision energy; this is a rather bizarre observation as the opposite is most often observed.

Vibrational Progressions

As shown in Figures 21 and 22 there are additional smaller peaks to the left of the main peaks. These are likely due to vibrational progressions. While it is true that Penning Ionization is typically an adiabatic process (i.e. an electronic transition with not vibrational transitions) transitions between vibrational states will occur. Looking at the spectra we can make out at least one $v=0 \rightarrow v'=1$ transition at 3.5eV. This observation is in agreement with an observation made by Vecchiocattivi⁴⁰. Vecchiocattivi observed the X state peak with two vibrational transitions. Unfortunately, there cannot be a comparison between the A state peak observed here and Vecchiocattivi's observation because the A state is missing in the spectra obtained in that paper.

⁴⁰ *Penning Ionization of N₂O Molecules by Be*(2^{3,1}S) and Ne*(³P_{2,0}) Metastable Atoms: A Crossed Beam Study*; Vecchiocattivi; J. Chem. Phys.; 122; 1643107-1; 2005

Conclusions

As discussed in the data analysis section there was a blue shift of 0.01eV for the X state and a blue shift of 0.04eV for the A state. As described in the theory section this indicates a blue shift. The presence of a blue shift corresponds to a resonance width that increases while $V_0(r)$ is repulsive as shown in Figure 8. This corresponds well to the expected theory. From this observation of a blue shift it is safe to say that as the Ne* atom approaches the N₂O molecule there is a repulsive interaction between the reagents up until the point of collision. This description is ignoring the lack of azimuthal symmetry for the N₂O molecule. However, this description does go well with the experiment because there is no way to orient the N₂O molecules during their reaction and hence the observed shift is due to a repulsive force that is an average of the repulsive force at each approach angle.

The observation that populations (and thus collision cross section) increases with increased collision energy is very interesting. This is counter to the observations with similar molecules such as CO₂. Past research in the Siska group⁴¹ has shown that PIES of CO₂ produces peaks that are red shifted. CO₂ also shows a decreasing collision cross section with increasing collision energy. This comparison illustrates a predicted trend: for collisions with repulsive interactions the collision cross section will increase with increased collision energy whereas for with attractive interactions the collision cross section will decrease with increased collision energy. This makes intuitive sense, an increased collision energy gives more molecules the kinetic energy needed to get past the

⁴¹ *PENNING IONIZATION OF SMALL MOLECULES BY METASTABLE NEON*, Thesis, Joe Noroski, 2007

centrifugal barrier and collide. Why do two structurally similar molecules (N_2O and CO_2) produce different forces in the reaction with Ne^* ? Though this topic merits a great deal more discussion, it could be due to the dipole moment of N_2O which CO_2 lacks (See appendix A-4).

Additionally, vibrational transitions of the form $v=0 \rightarrow v'=1$ and $v=0 \rightarrow v'=0$ are observed. This agrees with Vecchiocattivi's results for the X state peak. It is of course possible that other vibrational progressions are present however they cannot be resolved.

Appendix

A-1 Franck-Condon Approximation

One idea with regard to electronic transitions that I need to address is the Franck-Condon approximation. The idea is that in an electronic transition only the electron motion – not the nuclear motion – is important. The approximation treats the nuclei of the molecule as fixed because the electrons of a molecule are so much lighter than the nuclei. Because the electron is so much lighter, the electron will move much faster than the nuclei, resulting in relatively stationary nuclei. A quick look at the reduced mass of the hydrogen atom justifies this approximation.

This approximation is simple but allows several of the simplifications in this experiment. First, it is this approximation that allows the Franck-Condon principle to exist; without this approximation the vibrational and electronic wave functions are inseparable. Second, this approximation grants confidence that the ejected electrons are in fact good representatives of the orbitals they were ejected from. Were this approximation not true, the B⁺ molecule could rearrange its nuclei to a significant degree in the time it takes for an electron to be ejected.

The Franck-Condon Principle makes predictions about the intensities of the vibronic transitions we should observe. According to the Franck-Condon principle the intensity of a vibronic peak is proportional to the square of the overlap integral between the final and initial vibrational wave functions:

$$I = \int \Psi_{\text{final}} \Psi_{\text{initial}}^* d\tau \quad (20)$$

The most intense signals (most common transitions) will correspond to the greatest overlap of vibrational wave functions.

The Franck-Condon approximation says that electronic transitions occur quickly compared to the nuclear rearrangement. Thus the transitions that minimize nuclear movement will be favored the most in this reaction. This suggests that the $v=0 \rightarrow v'=0$ and $v=0 \rightarrow v'=1$ transitions will be the most common as they produce the least amount of nuclear rearrangement. From this we expect that the Penning Ionization reaction will produce mostly adiabatic transitions – an adiabatic transition is one in which there is no change in vibrational state, i.e. $v=0 \rightarrow v'=0$.

So what can this principle tell us about this particular experiment? Specifically, this principle will aid in the assignment of peaks to the N_2O spectrum. Penning Ionization reactions are, primarily, an adiabatic reaction ($v=0 \rightarrow v'=0$). This adiabatic transition will be the most heavily populated with the non-adiabatic transitions being less populated. This suggests that for each electron ionization energy we will see a large peak signifying the adiabatic transition and smaller peaks nearby signifying the non-adiabatic transitions.

A-2 Complex Potentials

As previously mentioned, the two potential model effectively describes the potential energy of the reaction components before and after a reaction. However, it would be nice if we knew how often or with what probability this transition occurred. A step in the right direction is to consider the Penning ionization reaction to be the decay of the $A^* + B$ system into the $A + B^+ + e^-$ system. The $A^* + B$ system is unstable and should be

expected to decay (at a small intermolecular distance of course). This decay can be accounted for mathematically by adding an imaginary part (the resonance width) to the potential $V_0(r)$ so that the potential of the reagent system is now $V_0(r) - i\Gamma(r)/2$.

Note that $\Gamma(R)$ is a function of R , the distance between A^* and B . In fact at the two potential diagram illustrates, $\Gamma(r)$ increases exponentially as the distance between A^* and B decreases. This suggests that as the two reagents approach each other the chance of decay (or reaction) increases. Likewise, at large r where A^* and B are far apart, the chance of decay is 0.

The need for $\Gamma(r)$ arises from the fact that using only a real potential leads to a "conservation of probability". From introductory quantum mechanics we can describe the time evolution of the probability of finding a particle in all space as:

$$d/dt(\text{integral over all space of: } \Psi^2 dx) = (\text{integral over all space of: } d/dt(\Psi^2) dx)$$

To work with this equation we need the Schrodinger equation which says:

$$\frac{d}{dt}\Psi = \frac{-ih\pi}{m} \cdot \frac{d^2}{dx^2}\Psi - iV\Psi \quad (21)$$

For a real V this will give the result of the time evolution of the probability of finding the particle in state $A^* + B$ is 0. If there is no imaginary component dP/dt should be zero.

However, if imaginary component, Γ is not zero, the probability is not conserved and for a constant Γ :⁴²

$$\frac{d}{dt}P = \frac{-2\pi}{h} \Gamma \cdot P \quad (22)$$

In the case of the two potential model the Γ part has a dependence on r . As the

⁴² *Introduction to Quantum Mechanics*; David Griffiths; Pearson Prentice Hall; 2nd Ed.; 2004; page 22; problem 1.15

molecules approach each other $\Gamma(R)/2$ slowly increases from 0. As the molecules move even closer together $\Gamma(r)$ increases exponentially, making the probability of reaction almost guaranteed as the molecules collide.

A-3 Vibrational Analysis of N₂O

N₂O is very similar to CO₂ and has four vibrational modes.⁴³ Like CO₂, N₂O has symmetric stretching mode, an anti-symmetric stretching mode and a doubly degenerate bending mode. During an electronic transition, each of these modes can be excited from the ground vibronic state ($v = 0$) to an excited electronic state and any number of vibrational states ($v' = 0, 1, 2, 3, \dots$). Transitions where the vibrational level remains in the ground state during the electronic transition are referred to as adiabatic transitions. Transitions that involve a change in vibrational states are referred to as non-adiabatic transitions.

Non-adiabatic transitions will occur when the positions of nuclei shift during an electronic transition. Such a shift will occur when an electron is ejected from strongly bonding orbitals or strongly anti-bonding orbitals. Similarly, adiabatic transitions will occur when electrons are ejected from non-bonding, weakly bonding, or weakly anti-bonding orbitals. Non-adiabatic transitions will possess higher energy - and subsequently give off electrons with lower kinetic energy - than their adiabatic counterparts. In this way the electronic spectrum will reflect these transitions. The vibrational splitting of the non-adiabatic transitions will help to distinguish them from the adiabatic transitions.

⁴³<http://cfa-www.harvard.edu/hitran/vibrational.html>

A-4 Properties of Target Molecule N₂O

For clarity it is necessary to discuss the structure of the target molecule, N₂O. N₂O, like CO₂, is a linear molecule with four vibrational modes. The vibrational modes occur at 2224cm⁻¹, 1285cm⁻¹, and 589cm⁻¹ (doubly degenerate).⁴⁴ The difference between the two molecules is their symmetry; CO₂ belongs to the point group D_{∞h} and N₂O belongs to the point group C_{∞h}. This will give N₂O a dipole moment which likely contributes to the repulsive force the molecule experiences during the Penning Ionization reaction with Ne*. Figure 23 shows the structure of N₂O and Figure 24 shows the molecular orbital diagram for N₂O. The HOMO of N₂O is a non-bonding orbital⁴⁵ (also true of N₂O⁺); thus if an electron is removed adiabatically from that orbital it will not affect the nuclear arrangement of the N₂O molecule.

⁴⁴ <http://cfa-www.harvard.edu/hitran/vibrational.html>

⁴⁵ *Handbook of HeI Photoelectron Spectra of Fundamental Organic Molecules*; K. Kimura, S. Katsumata, Y. Achiba, T. Yamazaki, S. Iwata; Halsted Press, New York; 1981, page 35

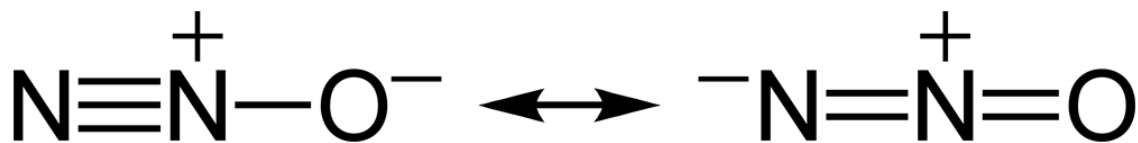


Figure 23: Lewis structure for N_2O . The asymmetry indicates a dipole moment that is lacking in CO_2 .⁴⁶

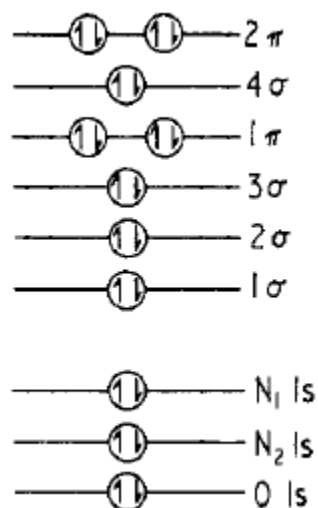


Figure 24: Electron configuration for N_2O . Electrons removed from the valence shell belong to non-bonding pi orbitals. Ionization of the 2π orbital produces the X state of N_2O . Ionization of the 4σ orbital produces the A state.⁴⁷

⁴⁶ Image from http://en.wikipedia.org/wiki/Nitrous_oxide

⁴⁷ *X-ray Emission Spectra of NH_3 and N_2O* ; J. Nordgren; Uppsala University, Sweden; J. Phys. B: Atom. Molec. Phys.; Vol 9; No. 2; 1976

A-5 List of Equipment

| Equipment | Brand and Model | Quantity |
|----------------------------------|-------------------------------|-----------------|
| Electron Analyzer | Comstock AC-901 160° | 1 |
| Einzel Lens | Comstock EL-301. | 1 |
| Electron Multiplier | K&M Electronics CERAMAX 7551m | 1 |
| Diffusion Pump (small) | Varian VHS-4 | 2 |
| Diffusion Pump (large) | Varian VHS-6 | 3 |
| Mechanical Pump (Primary Beam) | Welch Duo-Seal 1397 | 1 |
| Mechanical Pump (Secondary Beam) | Alcatel 2033C | 1 |
| Mechanical Pump (Main Chamber) | Alcatel 2033 | 1 |
| Mechanical Pump (HeI Lamp) | Alcatel M2004A | 2 |

References

- *Molecular-beam studies of Penning Ionization*, P.E. Siska, Rev. Mod. Phys., Vol 65, No. 2, April 1993; Page 337
- *Experimental Techniques in High-Energy Nuclear and Particle Physics*; Thomas Ferbel; 1991; World Scientific
- *The Collision Dependence of Penning Ionization of Nitrogen Molecules by Metastable helium as Determined by Electron Spectroscopy*; Dunlavy; PhD. Thesis; University of Pittsburgh; 1996
- *Penning Ionization and Related Processes*; Yenchu; Dept Chem; NY State University at Albany; 1984
- *Atomic and Molecular Beams: The State of the Art*; Roger Campargue; 2000
- *Plasma Physics and Engineering*; Alexander A. Fridman, Lawrence A. Kennedy; 2004; Taylor and Francis
- *Doubly Differential Reactive Scattering In Molecular Penning Ionization Systems*, 2005, Keerti Gulati, Univ. Pitt, Thesis
- *Principles of Instrumental Analysis*, Skoog, Holler, Nieman; Brooks/Cole; 5th Ed.
- *Classical Mechanics*; John Taylor; University Science Books; 2004
- *Introduction to Quantum Mechanics*; David Griffiths; Pearson Prentice Hall; 2nd Ed.; 2004
- *PENNING IONIZATION OF SMALL MOLECULES BY METASTABLE NEON*, Univ. Pitt , Thesis, Joe Noroski, 2007
- *Quantum Chemistry and Spectroscopy*; Thomas Engel; Pearson Education; 2006

- *Computation of Auto-Ionization Life Times via a Golden Rule*; W. H. Miller; Chem. Phys Letters.; Issue 4 Page 627; 1970
- *Theory of Penning Ionization*; W. H. Miller; J. Chem. Phys.; Vol 52; Number 7; 1970
- *Chemical Kinetics and Reaction Dynamics*, Upadhyay.
- *Magnetic Deflection Analysis of Supersonic Metastable Atom Beams*; Weisner and Siska; 1987; Rev. Sci. Instruments; 58; page 2124
- *Penning Ionization of N₂O Molecules by Be*(2^{3,1}S) and Ne*(³P_{2,0}) Metastable Atoms: A Crossed Beam Study*; Vecchiocattivi; J. Chem. Phys.; 122; 1643107-1; 2005
- *The temperature dependence of penning ionization electron energy spectra: He(2³S)-ar, N₂, NO, O₂, N₂O, CO₂*, Hotop, H., Kolb, E., Lorenzen, J., Journal of Electron Spectroscopy and Related Phenomena, 16 (3), pages 213-243, 1979
- ¹ *State-resolved collision energy dependence of Penning ionization cross sections for N₂ and CO₂ by He*2³*; Ohno, Takami, Mitsuke; Journal of Chemical Physics; Vol 94; page 2675; 1991
- F.M. Penning; *Naturwissenschaften*, 1927, **15**, 818
- *Handbook of HeI Photoelectron Spectra of Fundamental Organic Molecules*; K. Kimura, S. Katsumata, Y. Achiba, T. Yamazaki, S. Iwata; Halsted Press, New York; 1981
- *X-ray Emission Spectra of NH₃ and N₂O*; J. Nordgren; Uppsala University, Sweden; J. Phys. B: Atom. Molec. Phys.; Vol 9; No. 2; 1976
- <http://physics.nist.gov/>